SOME ANALYTICAL AND EXPERIMENTAL STUDIES OF LAMINAR PROPORTIONAL AMPLIFIERS

APRIL 1976

Prepared by

The Pennsylvania State University
Systems and Controls Laboratory
213 Mechanical Engineering Bldg
University Park, Pennsylvania 16802

Under Contract

DAAG-34-73-C-0213

U.S. Army Materiel Development
and Readiness Command
HARRY DIAMOND LABORATORIES
Adelphi, Maryland 20783

UNCLASSIFIED

SECURITY CLASSIFICATION OF THIS PAGE (When Data Entered)

(19) REPORT DOCUMENTATION PAGE

READ INSTRUCTIONS BEFORE COMPLETING FORM

(18) 1. REPORT NUMBER: HDL-CR-76-213-1

2. GOVT ACCESSION NO.

3. RECIPIENT'S CATALOG NUMBER

(6) 4. TITLE (and Subtitle): Some Analytical and Experimental Studies of Laminar Proportional Amplifiers

5. TYPE OF REPORT & PERIOD COVERED

6. PERFORMING ORG. REPORT NUMBER

(10) 7. AUTHOR(s): J. Lowen Shearer, Gary V. Smith

8. CONTRACT OR GRANT NUMBER(s): DAAG-34-73-C-0213 ~~~ DRCMS Code: 611102.11.71200

9. PERFORMING ORGANIZATION NAME AND ADDRESS: The Pennsylvania State University, 215 Mechanical Engineering Bldg., University Park, PA. 16802

10. PROGRAM ELEMENT, PROJECT, TASK AREA & WORK UNIT NUMBERS: Program Element: 6.11.02.A

11. CONTROLLING OFFICE NAME AND ADDRESS: Harry Diamond Laboratories, 2800 Powder Mill Road, Adelphi, MD 20783

(11) 12. REPORT DATE: April 1976

13. NUMBER OF PAGES: (12) 43 p.

14. MONITORING AGENCY NAME & ADDRESS (if different from Controlling Office)

15. SECURITY CLASS. (of this report): Unclassified

15a. DECLASSIFICATION/DOWNGRADING SCHEDULE

16. DISTRIBUTION STATEMENT (of this Report)

Approved for public release; distribution is unlimited

(15) DAAG-34-73-C-0213

17. DISTRIBUTION STATEMENT (of the abstract entered in Block 20, if different from Report)

(16) DH-1-T-161102-A-33-B

HDL-30233B

18. SUPPLEMENTARY NOTES

DA No.: 1T161102A33B

HDL Project No.: 30233B

19. KEY WORDS (Continue on reverse side if necessary and identify by block number)

Proportional Amplifier (Laminar)
Supply Characteristics
Input Characteristics
Transfer Characteristics
Output Characteristics
Pressure Noise Characteristics

20. ABSTRACT (Continue on reverse side if necessary and identify by block number)

This report presents the results of an analytical and experimental investigation of a pressure-controlled proportional amplifier which operates with a supply jet in the laminar flow regime. A mathematical model is developed which may be used for the prediction of the supply characteristics, input characteristics for three types of input signals, transfer characteristics, and output characteristics of the amplifier. Acceptable agreement is found to exist between theory and experimental data although theory predicts a slightly greater aspect ratio dependency than the data indicate. (More complete abstract found on page 3).

DD FORM 1473 EDITION OF 1 NOV 65 IS OBSOLETE

UNCLASSIFIED

ABSTRACT

This report presents the results of an analytical and experimental investigation of a pressure-controlled proportional amplifier which operates with a supply jet in the laminar flow regime. A mathematical model is developed which may be used for the prediction of the supply characteristics, input characteristics for three types of input signals, transfer characteristics, and output characteristics of the amplifier. Acceptable agreement is found to exist between theory and experimental data although theory predicts a slightly greater aspect ratio dependency than the data indicate.

In general, the data indicate that the normalized operating characteristics are relatively weak functions of the aspect ratio and Reynolds number over the investigated range, although a strong dependency of the operating characteristics on the mean control pressure was found to exist. Both the deflected-jet input resistance and pressure gain of the amplifier were found to decrease with increasing mean control pressure. It was also determined that a reduction in the setback of the control knife-edges results in an increase in the null input resistance as predicted by theory. A setback reduction of one-half to one-fourth the supply nozzle width was found to not decrease the linear range of operation of the amplifier. An experimental investigation of the differential output noise characteristics of the amplifier indicates a linear increase of noise with increasing aspect ratio and exponential growth of noise with increasing Reynolds number for a fixed bandwidth of noise measurement.

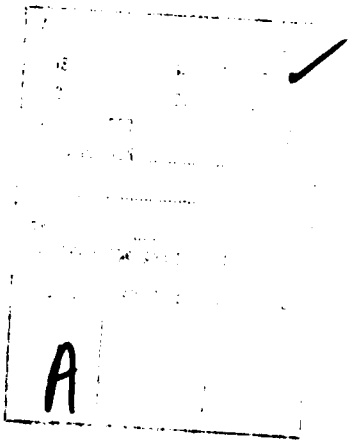

TABLE OF CONTENTS

LIST OF ILLUSTRATIONS

NOMENCLATURE

B'_{cc}	Control channel width
B'_{ra}	Average receiver channel width
B'_{ri}	Receiver inlet width
B'_{s}	Supply nozzle width
B'_{SB}	Setback of control knife-edge
C_{d}	Discharge coefficient
C_{fd}	Coefficient of fully developed friction factor
C_{vc}	Vena contracta coefficient
C_{θ}	Momentum flux discharge coefficient
D'_{cyl}	Diameter of cylinderical leading edge of splitter
G	Pressure gain
H'	Amplifier height
J'_{cr}	Control momentum flux incident upon receivers
J'_{sr}	Supply momentum flux incident upon receivers
k_{d}	Coefficient of Y_{d}
K_{l}	Pressure drop factor
L'_{c}	Axial distance from supply nozzle exit to control knife-edges
L'_{cc}	Control channel length
L'_{r}	Receiver channel length
L'_{T}	Axial distance from supply nozzle exit to receiver entrance
L'_{v}	Axial distance from control knife-edges to receiver entrance
L'_{th}	Supply nozzle throat length
L'_{vo}	Virtual origin length
N_{Rh}	Reynolds number, $V'_{sa}H'/\nu'$
N_{Rb}	Reynolds number, $V'_{sa}B'_{s}/\nu'$
P'_{b}	Bias pressure

P'_{bm}	Mean bias pressure $[P'_{b1} + P'_{b2})/2]$
P'_{c}	Control pressure
P'_{cm}	Mean control pressure $[P'_{c1} + P'_{c2})/2]$
P'_{kin}	Kinetic (i.e. dynamic) pressure of entrained flow
P'_{o}	Output pressure
P'_{on}	Null output pressure
P'_{r}	Receiver pressure
P'_{rn}	Null receiver pressure
P'_{s}	Supply pressure
$\Delta P'$	Pressure drop due to boundary layer growth
$\Delta P'_{of}$	Fluctuating component of the differential output pressure
Q'_{c}	Control volumetric flow rate
Q'_{cn}	Control volumetric flow rate for null operation
Q'_{d}	Volumetric flow rate through orifice formed by lateral displacement of supply jet
Q'_{o}	Output volumetric flow rate
Q'_{on}	Null output volumetric flow rate
Q'_{s}	Supply volumetric flow rate
R'_{b}	Incremental fluid resistance of null supply jet-control knife-edge orifice
$(R'_{b})_{app}$	Apparent fluid resistance of null supply jet-control knife-edge orifice
R'_{cc}	Incremental fluid resistance of control channel
$(R'_{cc})_{app}$	Apparent fluid resistance of control channel
R'_{d}	Incremental fluid resistance of orifice formed by lateral deflection of supply jet
R'_{i}	Input resistance
R'_{L}	Incremental load resistance
$(R'_{L})_{app}$	Apparent load resistance

R'_r	Incremental fluid resistance of receiver channel
$(R'_r)_{app}$	Apparent fluid resistance of receiver channel
v'	Velocity in boundary layer
V'_p	Potential core velocity of supply flow
V'_{sa}	Average exit supply velocity
x'	Coordinate parallel to axis of LPA
y'	Transverse coordinate of LPA
Y'_b	Incremental fluid admittance of null supply jet-control knife-edge orifice
y'_c	Lateral jet displacement at control knife-edge
Y'_d	Incremental fluid admittance of orifice formed by lateral deflection of supply jet
y'_r	Lateral jet displacement at inlet to receiver

Greek Symbols

δ	Incremental change
$\delta^{*\prime}$	Displacement thickness
δ'_t	Boundary layer thickness
ν'	Kinematic viscosity
ρ'	Fluid density
σ	Aspect ratio, H'/B'_s

Superscripts

'	Denotes dimensional quantity

Subscripts

BL	Blocked-load conditions
cv	converging section of supply nozzle
e	exit
i	inlet
1,2	Denotes opposing sides of inputs and outputs of LPA

1. INTRODUCTION

One of the primary components used in the design of fluidic control systems is the proportional amplifier. The type of proportional amplifier which has received the most attention is the jet-deflection amplifier (also known as the beam deflection amplifier) originally conceived by B. M. Horton in 1959. Early work on the jet-deflection amplifier was centered on a turbulent supply jet being deflected by the momentum of turbulent control jets.

The primary disadvantages of jet-deflection amplifiers which operate with turbulent supply jets are low gain, low signal-to-noise ratios and stability problems which primarily arise when large output loads are applied to the output ports of the amplifier. The low gain and low signal-to-noise ratios of the amplifier are primarily due to the nature of the turbulent supply jet. Both the gain and normalized pressure recovery are limited because of the rapid spread of a turbulent jet. In addition, the noise output of the amplifier is strongly related to the turbulent nature of the supply jet.

One approach to circumvent these problems associated with the jet-deflection amplifier is to operate with a laminar supply jet. If the supply jet Reynolds number at the exit of the supply nozzle is not too low, the spread of the laminar jet will be much less than a turbulent jet--resulting in an increase in both gain and normalized pressure recovery. Signal-to-noise ratios for jet-deflection amplifiers designed for operation with laminar supply jets would also be expected to be much greater than amplifiers designed for operation with turbulent jets.

The development of a jet-deflection amplifier which operates in the laminar flow regime is described by Manion and Mon,[1] Smith and Shearer,[2] Manion and Drzewiecki,[3] and Smith.[4] Since this is the final summary report required under this contract it will briefly review aspects of earlier reports and referenced literature which are pertinent and essential to the development of ideas, concepts and analysis employed in this research.

---

[1]Manion, F. M., and Mon, G., Fluerics: 33. Design and Staging of Laminar Proportional Amplifiers, Harry Diamond Laboratories-TR-1608, Adelphi, MD, 1972.

[2]Smith, G. V., and Shearer, J. L., Research Investigation on Laminar Proportional Amplifiers, Final Report Contract DAAG-39-72-C-0190, The Pennsylvania State University, University Park, PA., 1974.

[3]Manion, F. M., and Drzewiecki, T. M., Analytic Design of Laminar Proportional Amplifiers, Proceedings HDL Fluidics State-of-the Art Symposium, Adelphi, MD, 1974.

[4]Smith, G. V., An Analysis of Laminar Proportional Amplifiers, Ph.D. Thesis, The Pennsylvania State University, University Park, PA., 1975.

The work of Manion and Mon[1] describes the development of a laminar proportional amplifier (LPA) very similar to that shown in Fig. 1. This design, which has a setback of one half of the supply nozzle width, uses a pressure field to deflect the laminar supply jet. They report that a pressure field effectively deflects the laminar jet without disturbing the flow field whereas a momentum exchange design introduces noise.

The Reynolds number range in which the LPA should operate is limited by excessive jet spreading on the one hand and transition to turbulence on the other. Manion and Mon,[1] Smith and Shearer,[2] and Smith[4] report on the results of flow visualization studies and report that the device should operate properly in a Reynolds number range of approximately 700 to 1500 where the Reynolds number is based on the amplifier height and the average supply velocity. Smith and Shearer[2] and Smith[4] also report on the feasibility of operating the LPA with reduced setback.

Manion and Mon[1] present a control volume analysis for the static and dynamic pressure gain of the LPA. Their analysis, which is restricted to a push-pull input signal, relies in part on experimental data and does not include all of the effects of the bias pressure on the performance of the LPA. Their report also includes a method to properly stage the LPA.

Manion and Drzewiecki[3] present a fairly comprehensive analysis of the operating characteristics of an LPA. Their analytical investigation of the input characteristics, transfer characteristics and output characteristics are compared to data and, in general, acceptable agreement is found to exist. It is felt, however, that their analysis of the control port-supply jet interaction region does not include all of the bias pressure effects. Their analysis of the transfer characteristics is limited to blocked-load conditions at the output ports while their analysis of the output characteristics is limited to null supply jet operation. In addition, both the input characteristics and transfer characteristics are limited to push-pull input signals. Their paper also includes a dynamic analysis of the LPA as well as geometric configuration and contamination sensitivity problems.

---

[1]Manion, F. M., and Mon. G., Fluerics: 33. Design and Staging of Laminar Proportional Amplifiers, Harry Diamond Laboratories-TR-1608, Adelphi, MD, 1972.

[2]Smith, G. V., and Shearer, J. L., Research Investigation on Laminar Proportional Amplifiers, Final Report Contract DAAG-39-72-C-0190, The Pennsylvania State University, University Park, PA., 1974.

[4]Smith, G. V., An Analysis of Laminar Proportional Amplifiers, Ph.D. Thesis, The Pennsylvania State University, University Park, PA., 1975.

[3]Manion, F. M., and Drzewiecki, T. M., Analytic Design of Laminar Proportional Amplifiers, Proceedings HDL Fluidics State-of-the Art Symposium, Adelphi, MD, 1974.

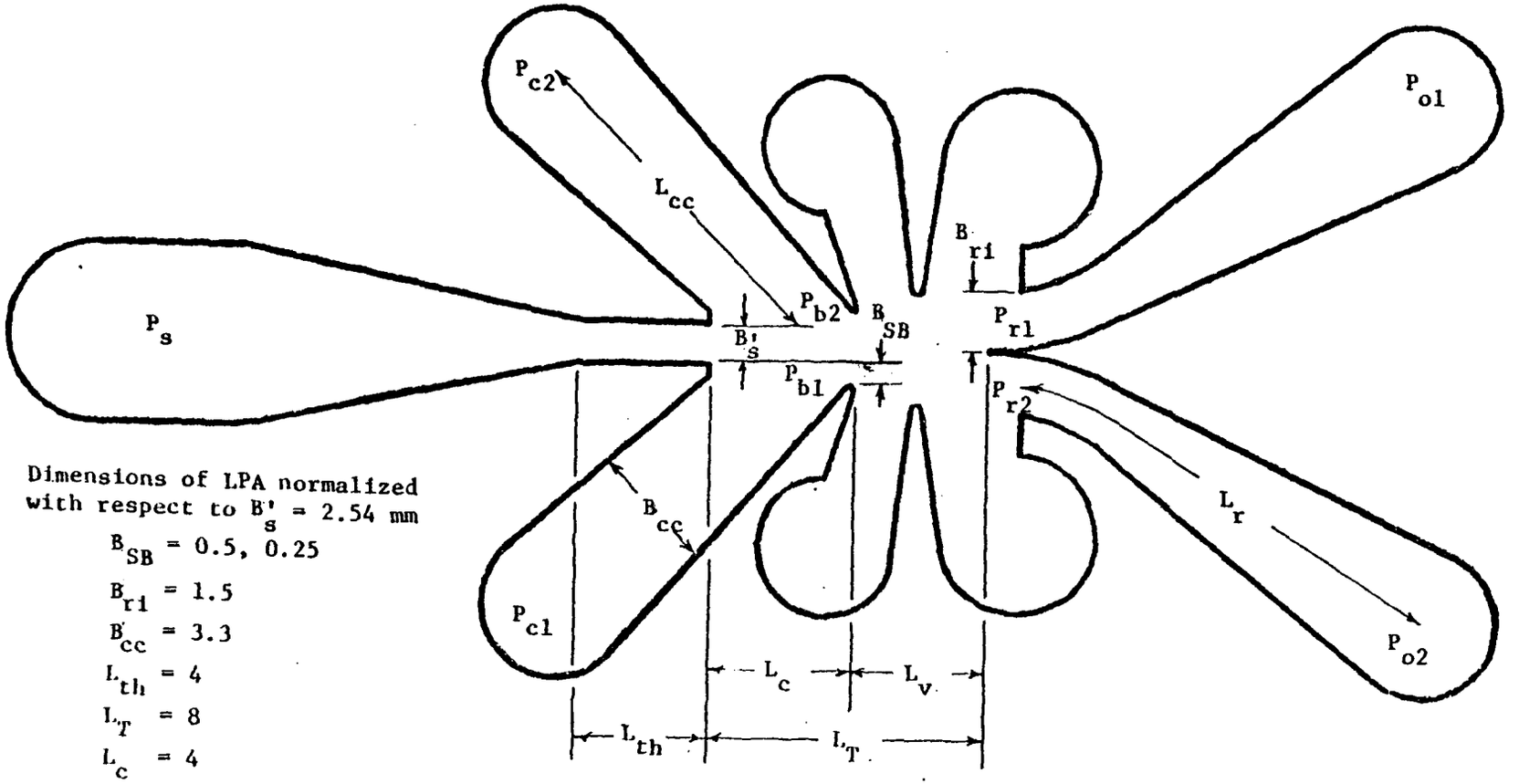

11

Dimensions of LPA normalized with respect to B'_s = 2.54 mm

B_{SB} = 0.5, 0.25

B_{ri} = 1.5

B_{cc} = 3.3

L_{th} = 4

L_T = 8

L_c = 4

L_v = 4

L_{cc} = 9

L_r = 14

Figure 1. Schematic of LPA used in this study.

The purpose of this paper is to report the results of an analytical and experimental investigation of the operating characteristics of the LPA shown in Fig. 1

2. MATHEMATICAL MODEL

In this section a mathematical model for the prediction of the operating characteristics of laminar proportional amplifiers is presented. In the formulation of this model primary consideration was given to developing a theory which, in addition to accurately predicting the operating characteristics of an LPA, would easily indicate the effects of various operating parameters and important geometric parameters. In addition it was deemed important to develop a mathematical model which could easily be used for different types of input signals commonly encountered in actual applications.

In this analysis primes are used to denote dimensional quantities while unprimed quantities denote dimensionless quantities. All pressures, flow rates, and length dimensions are normalized with respect to the supply pressure, supply flow rate and supply nozzle width respectively.

2.1 Supply Characteristics

The basic approach to this analysis of the pressure-flow characteristics of laminar flow in the supply nozzle of the LPA shown in Fig. 1 will be the determination of the pressure drop across the nozzle for a given volumetric flow rate.

The supply nozzle is composed of three separate geometric regimes: a parallel wall plenum chamber; a converging section; and a parallel wall throat section. Calculations indicate that the pressure drop across the relatively large cross sectional area plenum chamber is sufficiently small, as compared to the presssure drop across the converging section and the throat section, that it may be neglected without appreciable error.

For the converging section the inlet flow will be assumed to have a uniform velocity profile and the boundary layer growth will be determined through the use of von Karmen's momentum integral equation for two-dimensional incompressible boundary layers with an axial pressure gradient. Although the flow in the converging section is three-dimensional due to the presence of the bounding plates of the LPA, the growth of the boundary layer is assumed to be the same on the vertical walls as on the bounding plates and small enough so that two-dimensional flow may be assumed. The assumption of a suitable velocity distribution in the boundary layer ($v'=V'_p \sin[\pi y'/2\delta'_t]$) enables the momentum thickness of the boundary layer and the wall shear stress to be related to the displacement thickness of the boundary layer so that von Karmen's momentum integral equation may be expressed in non-dimensional form as

$$\delta^* V_p \frac{d\delta^*}{dx} + 4.65 (\delta^*)^2 \frac{dV_p}{dx} = \frac{1.51}{N_{Rb}} \qquad (1)$$

where V_p and both δ^* and x are normalized with respect to V'_{sa} and B'_s respectively.

The variation of the core velocity with axial distance is estimated from continuity for this converging nozzle as

$$V_p = \frac{1}{(5 - 0.4x)} \tag{2}$$

Substitution of Eqn. (2) and its derivative into Eqn. (1) yields

$$\frac{\delta^*}{(5 - 0.4x)} \frac{d\delta^*}{dx} + \frac{1.86}{(5 - 0.4x)^2} (\delta^*)^2 = \frac{1.51}{N_{Rb}} \tag{3}$$

If it is assumed that the displacement thickness increases proportionally to the square root of the ratio of the axial distance to the Reynolds number based on nozzle width (an assumption justified by Smith[4]), the displacement thickness at the end of the converging section is determined from Eqn. (3) to be

$$\delta_i^* = \frac{0.89}{(N_{Rb})^{\frac{1}{2}}} \tag{4}$$

The core velocity at the end of the converging section is obtained from continuity as

$$V_{pi} = \frac{1}{(1 - 2\delta_i^*)(1 - 2\delta_i^*/\sigma)} \tag{5}$$

The pressure drop in the converging section for the case with boundary layer growth is greater than that would occur with ideal hydrodynamic flow. The increase in the pressure drop is found by applying Bernoulli's equation to a centerline stream tube which yeilds

$$\frac{(\Delta P')_{cv}}{\frac{1}{2}\rho' V'^2_{sa}} = (V_{pi})^2 - 1 \tag{6}$$

The pressure drop in the throat section is obtained from an analysis of laminar flow development in rectangular channels with a uniform velocity profile at the inlet. Schlicting[5] has shown that the difference between the core velocity and the average velocity in the entry region of a parallel plate channel is proportional to the square root of the axial distance. This relationship continues to apply in the entry region of a rectangular channel where the interaction between boundary layers is negligible. Applying Bernoulli's equation to the centerline stream tube enables this relationship

---

[4]Smith, G. V., An Analysis of Laminar Proportional Amplifiers, Ph.D. Thesis, The Pennsylvania State University, University Park, PA. 1975.

[5]Schlicting,H. Boundary Layer Theory, McGraw-Hill Book Co., Inc., N.Y., 1968.

to be expressed as

$$\frac{(\Delta P')}{\frac{1}{2}\rho' V'^{2}_{sa}} = C_1 \left[\frac{1 + \sigma}{2(\sigma)^{\frac{1}{2}}} \right] \left[\frac{x}{N_{Rh}} \right]^{\frac{1}{2}} \tag{7}$$

The constant of proportionality, C_1, is determined from the experimental data of Sparrow et al.[6] as approximately equal to 14. It is noted that this value is close to the value of 13.74 obtained by Shapiro et al.[7] for developing flow in tubes.

The analysis of the pressure drop in the throat section is made slightly more complicated due to the fact that the velocity profile entering the throat section is not uniform but is partially developed due to boundary layer growth in the converging section. Thus a "virtual origin length", defined as the entrance length of a rectangular channel over which the pressure drop due to boundary layer growth is the same as in the converging section, is obtained by substitution of Eqn. (6) into Eqn. (7) which yields

$$L_{vo} = \frac{N_{Rh}}{196} \left[\frac{2(\sigma)^{\frac{1}{2}}}{1 + \sigma} \right] [(V_{pi})^2 - 1] \tag{8}$$

It should be noted that for Reynolds numbers (based on amplifier height) from 600 to 1500 and for aspect ratios of 0.5 to 2.0, Eqn. (8) varies by less than 10 per cent from a "virtual origin length" of 0.36.

The total pressure drop in the supply nozzle is that due to the boundary layer growth plus that required to accelerate the fluid under ideal hydrodynamic flow conditions to the average supply velocity. Thus the total pressure drop is given as

$$\frac{P'_s - P'_b}{\frac{1}{2}\rho' V'^{2}_{sa}} = 1 + \frac{(\Delta P')}{\frac{1}{2}\rho' V'^{2}_{sa}} \tag{9}$$

The supply nozzle discharges coefficient is defined from the relation

$$Q'_s = C_d H' B'_s \left[\frac{2(P'_s - P'_b)}{\rho'} \right]^{\frac{1}{2}} \tag{10}$$

---

[6] Sparrow, E. M., Hixon, C. W., and Shavit, G., Experiments on Laminar Flow Development in Rectangular Ducts, Trans. ASME, Journal of Basic Engineering, Vol. 89, 1967.

[7] Shapiro, A. H., Siegel, R., and Kline, S. J., Friction Factors in the Laminar Entry Region of a Smooth Tube, Proc. U. S. Nat. Congr. Appl. Mech., 1954.

Substituting Eqns. (7) and (9) into Eqn. (10) and solving for the discharge coefficient yields

$$C_d = \left[\frac{1}{1 + 14 \left[\frac{1 + \sigma}{2(\sigma)^{\frac{1}{2}}} \right] \left[\frac{L_{vo} + L_{th}}{N_{Rh}} \right]^{\frac{1}{2}}} \right]^{\frac{1}{2}} \tag{11}$$

It is interesting to note that the term, $(1+\sigma)/2(\sigma)^{\frac{1}{2}}$, varies by a maximum of 6 per cent from a value of unity for aspect ratios of 0.5 to 2.0. Thus it is noted that the discharge coefficient is primarily determined by the Reynolds number based on amplifier height.

It should be noted that Eqn.(11) is based on the experimental data of Sparrow et al.[6] and although strictly valid only near the entrance of the channel, may be applied without appreciable error for

$$N_{Rh} > 65(L_{vo} + L_{th}) \left[\frac{1 + \sigma}{2(\sigma)^{\frac{1}{2}}} \right]^2 \tag{12}$$

For Reynolds numbers less than that indicated by Eqn. (12) an expression for the pressure drop for fully developed flow in channels with an entrance length correction should be used. Smith[4] gives such an expression for low Reynolds numbers as well as an expression for the discharge coefficient when the Reynolds number is based on the exit potential core velocity as opposed to the average exit velocity.

If it is assumed that the boundary layer thickness is approximately the same on all sides at the exit of the supply nozzle, the displacement thickness at the nozzle exit is given as

$$\delta_e^* = \frac{1 + \sigma}{4} - \left[\left[\frac{1 + \sigma}{4} \right]^2 - \frac{\sigma}{4} [\, 1 - C_d] \right]^{\frac{1}{2}} \tag{13}$$

The momentum flux discharge coefficient, C_θ, is obtained by reducing the nozzle dimensions by the sum of the displacement thickness and the momentum thickness. If it is assumed that the pressure gradient at the exit of the nozzle is negligible, the ratio of the displacement thickness to the momentum thickness is 2.59. The momentum flux discharge coefficient may therefore be expressed as

---

[6] Sparrow, E. M., Hixon, C. W., and Shavit, G., Experiments on Laminar Flow Development in Rectangular Ducts, Trans. ASME, Journal of Basic Engineering, Vol. 89, 1967.

[4] Smith, G. V., An Analysis of Laminar Proportional Amplifiers, Ph.D. Thesis, The Pennsylvania State University, University Park, PA. 1975.

$$C_\theta = [1 - 2.77\ \delta_e^*]\ [1 - 2.77\ \delta_e^*/\sigma] \tag{14}$$

2.2 Input Characteristics

The mathematical model for the determination of the input characteristics of the LPA is based on a lumped parameter analysis of the input flow field when the supply jet is in the centered (i.e. null) position. The resulting flow equations are then linearized for the input characteristics when the jet is deflected due to a lateral pressure gradient.

Figures 2 and 3 present the fluid circuit diagrams for the supply jet in the null position and in the deflected position respectively. The subscripts 1 and 2 denote opposing control ports.

In Fig. 2 P_c is the control pressure applied to the control port, Q_c is the control flow rate, P_b is the bias pressure existing at the supply nozzle exit and P_v is the vent pressure. All pressures in this and succeeding sections will be gage pressures measured relative to the vent pressure.

In Fig. 3 the δ's are used to denote small changes of the variables from their mean or null operating value. The change in control flow rate, δQ_c, is due to the difference between the change of control pressure, δP_c, and the change of bias pressure, δP_b. The change in the null control flow rate, δQ_{cn}, is due to a change in the bias pressure while δQ_d is the incremental flow rate through the area formed by the lateral displacement of the supply jet. It should be noted that δQ_d may be either plus or minus depending on the direction of the lateral displacement of the supply jet.

The apparent resistance of the control channel, $(R_{cc})_{app}$, is obtained from the pressure-flow characteristics of laminar flow in rectangular channels which includes both fully developed losses and entrance losses associated with developing flow. In normalized form this may be expressed as

$$P_c - P_b = (R_{cc})_{app}\ Q_c \tag{15}$$

where

$$(R_{cc})_{app} = \frac{C_{fd} L_{cc} C_d^2}{4 B_{cc} N_{Rh} \sigma} \left[1 + \frac{\sigma}{B_{cc}}\right]^2 + K_1 \left[\frac{C_d}{B_{cc}}\right]^2 Q_c \tag{16}$$

Typical experimental values of C_{fd} and K_1 from Sparrow et al.[6] are given as

---

[6] Sparrow, E. M., Hixon, C. W., and Shavit, G., Experiments on Laminar Flow Development in Rectangular Ducts, Trans. ASME, Journal of Basic Engineering, Vol. 89, 1967.

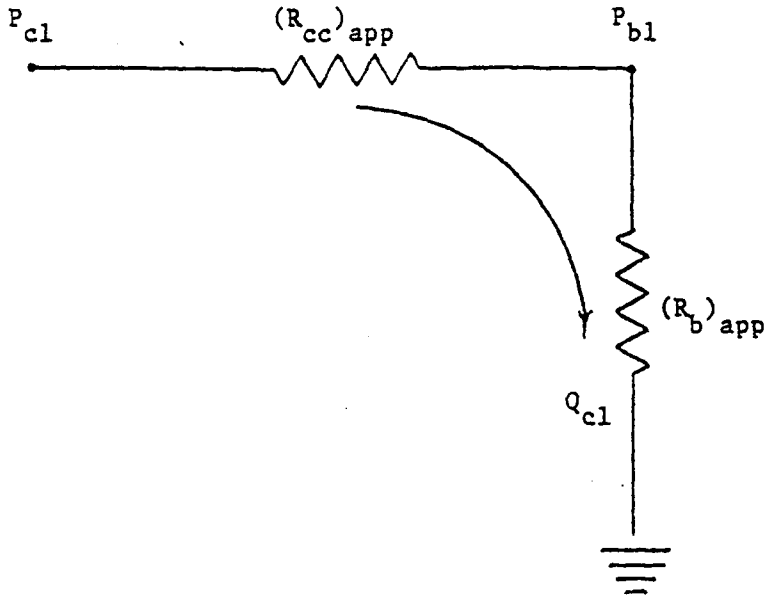

Figure 2 Control port region fluid circuit diagram for supply jet in null position

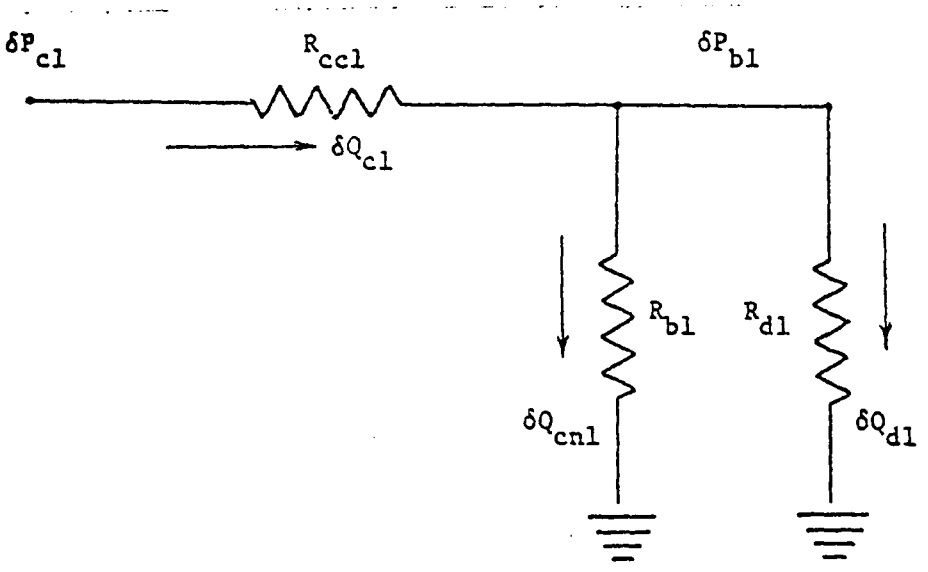

Figure 3. Control port region fluid circuit diagram for deflected supply jet.

$\sigma = 0.5; \quad C_{fd} = 62.2, \quad K_1 = 0.99$

$\sigma = 0.2; \quad C_{fd} = 76.3, \quad K_1 = 0.89,$

while analytical values of C_{fd} may be obtained from Han.[8]

The incremental resistance of the control channel, R_{cc}, defined as the slope of the pressure-flow characteristic at a given operating condition is obtained by differentiation of Eqn. (15) (using Eqn. (16) for $(R_{cc})_{app}$) with respect to Q_c which yeilds

$$R_{cc} = \frac{C_{fd} L_{cc} C_d^2}{4 B_{cc} N_{Rh} \sigma} \left[1 + \frac{\sigma}{B_{cc}}\right]^2 + 2K_1 \left[\frac{C_d}{B_{cc}}\right]^2 Q_c \qquad (17)$$

The pressure-flow characteristics for the region at the end of the control port channel when the supply jet is in the null position is obtained by modeling the area bounded by the control knife-edge, supply jet and the top and bottom plates as an orifice. The analysis of this orifice area is complicated because of the necessity of defining an effective jet width at the axial location of the control knife-edges and the dependency of the jet width on both the bias pressure and the spreading of the laminar jet. It is also noted that the flow rate through this orifice is not zero when the pressure drop across the orifice is zero but is equal to the rate of control flow entrained by that side of the supply jet.

Smith[4] discusses the effect of the bias pressure on the width of the supply jet and uses a simplified approach which employs an effective pressure drop to account for the complex nonlinear relationship that exists between the total flow and the entrainment and pressure drop factors. He states that the flow rate through the orifice may be expressed as

$$Q_c = \left[\frac{C_{vc} B_{SB} + 0.25 P_b}{C_d}\right] \left[P_b + P_{kin}\right]^{\frac{1}{2}} \qquad (18)$$

where

$$P_{kin} = \frac{L_c \sigma}{2 N_{Rh}} \left[\frac{C_d^2}{C_{vc} B_{SB}}\right]^2 \qquad (19)$$

---

[8] Han, L. S., Hydrodynamic Entrance Lengths for Incompressible Laminar Flow in Rectangular Ducts, Trans. ASME, Journal of Applied Mechanics, Vol. 82, 1960.

[4] Smith, G. V., An Analysis of Laminar Proportional Amplifiers, Ph.D. Thesis, The Pennsylvania State University, University Park, PA., 1975.

The first term in brackets in Eqn. (18) is the effective area of the orifice normalized with respect to the effective area of the supply nozzle exit. The term C_{vc} is a coefficient to account for the vena contracta effect in this orifice which is taken as equal to 0.75 from an inviscid analysis by Ehrich[9] for vena contracta coefficients in two-dimensional needle valves with an input angle of 45°. The increase in this orifice area with increasing bias pressure as indicated by Eqn. (18) was observed in flow visualization studies carried out by Smith[4].

The second term in brackets is the effective pressure drop across the orifice which consists of the bias pressure, P_b, and the dynamic pressure of the entrained flow rate, P_{kin}. An estimate of the entrained flow rate is obtained from Eqn. (18) when the bias pressure is zero.

Defining the apparent resistance of the control knife-edge orifice, $(R_b)_{app}$, as the ratio of the pressure drop across the orifice to the flow rate through the orifice yields

$$(R_b)_{app} = \frac{C_d P_b}{[C_{vc} B_{SB} + 0.25\ P_b]\ [P_b + P_{kin}]^{\frac{1}{2}}} \tag{20}$$

The incremental resistance of the control knife-edge orifice is obtained by differentiation of Eqn. (18) with respect to P_b which yields,

$$R_b = \frac{1}{Y_b} = \frac{8C_d\ [P_b + P_{kin}]^{\frac{1}{2}}}{4\ C_{vc} B_{SB} + 3\ P_b + 2\ P_{kin}} \tag{21}$$

In Eqn. (21) Y_b is the incremental admittance of the control knife-edge orifice. Both the apparent resistance and incremental resistance of the control knife-edge orifice are noted to be strong functions of the bias pressure.

The input characteristics for the supply jet in the null position is given as

$$P_c = [(R_{cc})_{app} + (R_b)_{app}]\ Q_c \tag{22}$$

where $(R_{cc})_{app}$ and $(R_b)_{app}$ are given by Eqns. (16) and (20) respectively.

---

[9]Ehrich, F. F., Some Hydrodynamic Aspects of Valves, ASME Paper No. 55--A-114, 1955.

[4]Smith, G. V., An Analysis of Laminar Proportional Amplifiers, Ph.D. Thesis, The Pennsylvania State University, University Park, PA., 1975.

It is noted, however, that the apparent resistance of the control channel is a function of the control flow rate while the apparent resistance of the control knife-edge orifice is a function of the bias pressure. The most straight forward procedure for the determination of the null input characteristics for given operating conditions is to determine the control flow rate for a given bias pressure from Eqn. (18). The corresponding control pressure is then easily obtained from Eqn. (15) for the given bias pressure and the calculated flow rate.

Before the deflected-jet input characteristics can be obtained, it is necessary to determine the relationship between the supply jet deflection and the differential pressure gradient existing across the supply jet. A fluid particle, upon exiting from the supply nozzle, undergoes a transverse acceleration due to the transverse pressure gradient acting upon it. Assuming that each fluid particle in the supply jet at a given axial location has undergone the same transverse displacement, that the axial jet velocity is essentially constant over the control port region and that the transverse pressure gradient is linear, Smith[4] has shown that the lateral jet displacement, y_c, at the end of the control port region is given by

$$y_c = \frac{L_c^2 (P_{b1} - P_{b2})}{4 C_\theta (1 - P_{bm})} \tag{23}$$

The flow rate through the additional orifice formed by the lateral displacement of the supply jet, Q_d, is given by

$$Q_d = \frac{y_c P_{bm}^{\frac{1}{2}}}{C_d} \tag{24}$$

Adopting the sign convention that a positive jet displacement results in a flow rate out of the control port region yields

$$Q_{d1} = \frac{L_c^2 P_{bm}^{\frac{1}{2}}}{4 C_d C_\theta (1 - P_{bm})} [P_{b1} - P_{b2}] \tag{25}$$

Perturbation of Eqn. (25) for small changes in the bias pressure yields

$$\delta Q_{d1} = Y_{d1} \delta P_{b1} \tag{26}$$

---

[4]Smith, G. V., An Analysis of Laminar Proportional Amplifiers, Ph.D. Thesis, The Pennsylvania State University, University Park, PA., 1975.

where

$$Y_{d1} = \frac{1}{R_{d1}} = k_d \left[1 - \frac{\delta P_{b2}}{\delta P_{b1}}\right] \tag{27}$$

and

$$k_d = \frac{L_c^2 P_{bm}^{\frac{1}{2}}}{4C_d C_\theta (1-P_{cm})} \tag{28}$$

The term k_d is a deflection coefficient of the admittance, Y_{d1}, and, although it is the same for each control port, it is a strong function of the bias pressure. The admittance is also observed to depend on the variation of P_{b2} with P_{b1} (i.e. $\delta P_{b2}/\delta P_{b1}$) indicating a dependency on the type of input signal applied to the symmetrically opposed control ports.

Solving the fluid circuit shown in Fig. 3 for the deflected-jet input resistance yields

$$R_{i1} = \frac{\delta P_{c1}}{\delta Q_{c1}} = \frac{1 + R_{cc}(Y_b + Y_{d1})}{Y_b + Y_{d1}} \tag{29}$$

As previously noted the admittance, Y_{d1}, and thus the deflected-jet input resistance, R_{i1}, of control port 1 depends on the nature of the sources used to provide the input signals applied to the symmetrically opposed control ports. This is due to the cross-coupling existing between the control ports provided by the supply jet. Smith[4] has analyzed three different types of input signals and has determined the resulting deflected-jet input resistance for control port 1 when it is driven by an ideal pressure or flow source. The resulting expressions are given as:

Case I, $\delta P_{c2} = -\delta P_{c1}$; (Ideal push-pull pressure sources)

$$R_{i1} = \frac{1 + R_{cc}(Y_b + 2k_d)}{Y_b + 2k_d} \tag{30}$$

Case II, $\delta P_{c2} = 0$; (Control port 2 driven by ideal pressure source held constant)

$$R_{i1} = \frac{1 + R_{cc}[2(Y_b + k_d) + R_{cc}Y_b(Y_b + 2k_d)]}{Y_b + k_d + R_{cc}Y_b(Y_b + 2k_d)} \tag{31}$$

---

[4]Smith, G. V., An Analysis of Laminar Proportional Amplifiers, Ph.D. Thesis, The Pennsylvania State University, University Park, PA., 1975.

Case III, $\delta Q_{c2} = 0$; (Control port 2 driven by ideal flow source held constant)

$$R_{i1} = \frac{Y_b + k_d + R_{cc} Y_b (Y_b + 2 k_d)}{Y_b (Y_b + 2 k_d)} \tag{32}$$

Smith[4] has also analyzed and developed an expression for the degree of cross-coupling existing between the control ports.

2.3 Transfer Characteristics

The transfer characteristics are analyzed by determining the pressure gain of the LPA under blocked-load conditions. The receiver pressure, P_r, is defined as the pressure existing at the entrance to the receivers while the output pressure, P_o is defined as the pressure existing at the output ports of the LPA. The pressure gain, G, of the LPA is defined as the change of differential output pressure divided by the change of differential input control pressure. For a small-signal analysis this is expressed as

$$G = \frac{\delta P_{o1} - \delta P_{o2}}{\delta P_{c1} - \delta P_{c2}} \tag{33}$$

The notation of control ports 1 and 2 and receivers 1 and 2 is such that a positive differential input signal results in a positive differential output signal.

Under blocked-load conditions the flow through each receiver is zero so that the receiver pressure is equal to the output pressure. The blocked-load pressure gain, G_{BL}, is then given as

$$G_{BL} = \frac{(\delta P_{o1} - \delta P_{o2})_{BL}}{\delta P_{c1} - \delta P_{c2}} = \frac{(\delta P_{r1} - \delta P_{r2})_{BL}}{\delta P_{c1} - \delta P_{c2}} \tag{34}$$

Equation (34) may be expressed as

$$G_{BL} = \left[\frac{(\delta P_{r1} - \delta P_{r2})_{BL}}{\delta y_r} \right] \left[\frac{\delta y_r}{\delta P_{b1} - \delta P_{b2}} \right] \left[\frac{\delta P_{b1} - \delta P_{b2}}{\delta P_{c1} - \delta P_{c2}} \right] \tag{35}$$

The first term in brackets in Eqn. (35) is the change in differential output pressure for a change in the lateral jet displacement at the entrance of the receivers. Smith[4] analyzes this term on the basis that the pressure at

---

[4] Smith, G. V., An Analysis of Laminar Proportional Amplifiers, Ph.D. Thesis, The Pennsylvania State University, University Park, PA., 1975.

the entrance of the receiver is determined by the net x-momentum flux incident upon the receiver entrance. Noting that the total incident momentum flux is equal to the sum of the supply momentum flux and the control momentum flux minus momentum flux losses due to shear effects, he perturbs the resulting equations to obtain

$$\frac{(\delta P_{r1} - \delta P_{r2})BL}{\delta y_r} = \frac{4}{B_{ri}} \left[J_{sr} - \frac{J_{cr} L_c}{2L_T - L_c} \right] \tag{36}$$

where the momentum influx at the receiver entrance due to the supply flow is given by

$$J_{sr} = C_\theta \left[1 - \frac{P_{bm}}{2}\right] - \frac{8C_d L_T}{N_{Rh}\sigma} - 1.34 \left[\frac{C_d D_{cyl}\sigma}{N_{Rh}}\right]^{1/2} \tag{37}$$

and the momentum influx at the receiver entrance due to the control flow is given by

$$J_{cr} = \left[2C_{vc}B_{SB} + \frac{P_{bm}}{2}\right] \left[P_{bm} - \frac{8C_d P_{bm}^{1/2}}{N_{Rh}\sigma}\right] \tag{38}$$

Both J_{sr} and J_{cr} are normalized with respect to the momentum efflux from the supply nozzle for ideal hydrodynamic flow.

The decrease in the blocked-load receiver pressure gain given by Eqn. (36) with increasing mean bias pressure is due to the reduction of supply momentum flux with increasing bias pressure and asymmetry of the flow past the control knife-edges when the supply jet is deflected.

The second term in brackets in Eqn. (35) is the change in lateral jet displacement at the receiver entrance for a change in lateral pressure difference existing across the supply jet. Assuming that the supply jet travels in a straight line after being deflected an amount y_c over the control port region, Smith[4] evaluates this term as

$$\frac{\delta y_r}{\delta P_{b1} - \delta P_{b2}} = \frac{2L_T L_c - L_c^2}{4C_\theta (1 - P_{bm})} \tag{39}$$

The third term in brackets in Eqn. (35) is the change in differential bias pressure for a change in differential control pressure and is obtained from the fluid circuit diagram in Fig. 3 as

$$\frac{\delta P_{b1} - \delta P_{b2}}{\delta P_{c1} - \delta P_{c2}} = \frac{1}{1 - R_{cc}(Y_b + 2k_d)} \tag{40}$$

---

[4] Smith, G. V., An Analysis of Laminar Proportional Amplifiers, Ph.D. Thesis, The Pennsylvania State University, University Park, PA., 1975.

Substitution of Eqns. (36), (39) and (40) into Eqn. (35) yields an expression for the blocked-load pressure gain as

$$G_{BL} = \frac{\left[J_{sr} - \frac{L_c J_{cr}}{2L_T - L_c} \right] \left[\frac{2L_T L_c - L_c^2}{C_\theta B_{ri}(1 - P_{bm})} \right]}{1 + R_{cc}[Y_b + 2\ k_d]} \tag{41}$$

As previously noted, the first term in brackets in the numerator decreases with increasing bias pressure while the second term in brackets is noted to increase with increasing bias pressure. Calculations indicate that the bias pressure effects on these two terms tend to cancel out so that a reasonable estimate of the numerator can be obtained by evaluating it for zero bias pressure. However, the denominator of Eqn. (41) is noted to be a strong function of the bias pressure--increasing with increasing bias pressure. Thus Eqn. (41) indicates that the pressure gain of the LPA under blocked-load conditions should decrease with increasing bias pressure. Because of the reduction in normalized shear losses with increasing Reynolds number, the gain should increase with increasing Reynolds number for a given aspect ratio. For a given Reynolds number (based on amplifier height) the sum of the normalized shear losses decreases with increasing aspect ratio-indicating larger pressure gains with higher aspect ratios.

2.4 Output Characteristics

The output characteristics of the LPA are analyzed by determining the output pressure-flow characteristics for one of the receivers as the applied load on the output port is varied for a particular value of differential control pressure.

The pressure at the entrance of the receiver, P_{rnl}, is the "driving" pressure or "source" pressure for the output flow under null conditions, Q_{onl}. When the load resistance applied to the LPA is infinity, the flow through the receiver channel is zero and the pressure at the entrance to the receivers is determined by the fact that all of the incident x-momentum flux is converted into y-momentum flux. As the loading on the LPA is reduced, flow is allowed to enter the receiver channel reducing the amount of x-momentum flux that is converted into y-momentum flux. Thus the "source" pressure decreases as the load resistance is decreased.

The relationship between the pressure at the receiver entrance for a given output flow and the pressure at the receiver entrance for blocked-load conditions may be obtained by making the assumption that the momentum flux incident upon the receivers is evenly distributed. The amount of x-momentum flux converted into y-momentum flux is then given by the difference between the x-momentum flux incident upon the receiver and the momentum flux entering the receiver channel. This is expressed as

$$P_{rnl} = \frac{J_{sr} + J_{cr}}{B_{ri}} - 2\left[\frac{C_d}{B_{ri}}\right]^2 Q_{onl}^2 \tag{42}$$

The relationship between the null receiver pressure and the null output pressure is obtained from the pressure drop for laminar flow in rectangular channels as

$$P_{rn1} - P_{on1} = (R_{r1})_{app} Q_{on1} \tag{43}$$

where

$$(R_{r1})_{app} = \frac{C_{fd} L_r C_d^2}{4 B_{ra} N_{Rh} \sigma} \left[1 + \frac{\sigma}{B_{ra}} \right]^2 + K_1 \left[\frac{C_d}{B_{ri}} \right]^2 Q_{on1} \tag{44}$$

Solving Eqns. (42) and (43) yields the desired null output pressure-flow characteristics as

$$P_{on1} = \frac{J_{sr} + J_{cr}}{B_{ri}} - \left[2 \left[\frac{C_d}{B_{ri}} \right]^2 Q_{on1} + (R_{r1})_{app} \right] Q_{on1} \tag{45}$$

The deflected-jet output characteristics under blocked-load conditions may be easily obtained from the definition of the blocked-load pressure gain which results in

$$P_{o1} = P_{on1} + \frac{G_{BL} [\delta P_{c1} - \delta P_{c2}]}{2} \tag{46}$$

Smith[4] also presents a linearized analysis of the variation of the pressure gain with equal resistive loads applied to the output ports. His equation for the pressure gain is then given as

$$\left[\frac{G}{G_{BL}} \right] = \frac{1}{1 + \dfrac{4 \left[\dfrac{C_d}{B_{ri}} \right]^2 Q_{on} + R_r}{R_L}} \tag{47}$$

where

$$R_r = \frac{C_{fd} L_r C_d^2}{4 B_{ra} N_{Rh} \sigma} \left[1 + \frac{\sigma}{B_{ra}} \right]^2 2 K_1 \left[\frac{C_d}{B_{ri}} \right]^2 Q_{on} \tag{48}$$

---

[4] Smith, G. V., An Analysis of Laminar Proportional Amplifiers, Ph.D. Thesis, The Pennsylvania State University, University Park, PA., 1975.

As would be expected, the pressure gain of the LPA approaches the blocked-load pressure gain as the applied resistive loads approach infinity.

It is important to note that the normalized pressure gain given by Eqn. (47) is a strong function of the null output flow rate (note that R_r is also a function of Q_{op}). It is therefore necessary to determine the null output flow rate for a given resistive load applied to the output ports as discussed by Smith.[4] As would be expected it is therefore necessary to know the complete pressure-flow characteristics of the load to be driven by the LPA before the pressure gain can be determined.

Smith[4] has also presented an analysis of the dynamic input impedance of the LPA for three types of input signals as well as an analysis of the dynamic pressure gain of the LPA.

3. EXPERIMENTAL RESULTS

In this section the results of an experimental investigation of the static operating characteristics of an LPA are presented and compared to theory. The dimensions of the LPA used in this study are shown In Fig. 1. Unless otherwise noted all data were taken using a model with a setback of one-half of the supply nozzle width. In order to investigate the effects of reduced setback on amplifier performance, some data were taken using a model with a setback of one-fourth of the supply nozzle width.

In order to obtain easily measurable pressures and flow rates, a hydraulic fluid (MIL-H-5606) was used as the working fluid. Flow rates were measured with calibrated variable area flow meters while pressures were measured manometrically.

3.1 Supply Characteristics

Figure 4 presents the supply pressure-flow characteristics for an aspect ratio of 0.56 and for nozzle exit pressures of up to 30 per cent of the supply pressure. Also shown on this figure is the predicted pressure-flow characteristic from Eqn. (10). Good agreement between theory and experimental data is noted to exist.

As previously noted, the discharge coefficient is primarily determined by the Reynolds number based on amplifier height. Since the supply flow rate is directly proportional to this Reynolds number, one would expect that if the supply flow rate were plotted versus the difference between the supply pressure and the nozzle exit pressure times the square of the aspect ratio, the data would collapse into a single curve. This data is presented in Fig. 5 and it is observed that the data essentially does collapse into a single curve. Also shown on this figure are the predicted pressure-flow characteristics for an aspect ratio of 1. The predicted curves for each of

---

[4] Smith, G. V., An Analysis of Laminar Proportional Amplifiers, Ph.D. Thesis, The Pennsylvania State University, University Park, PA., 1975.

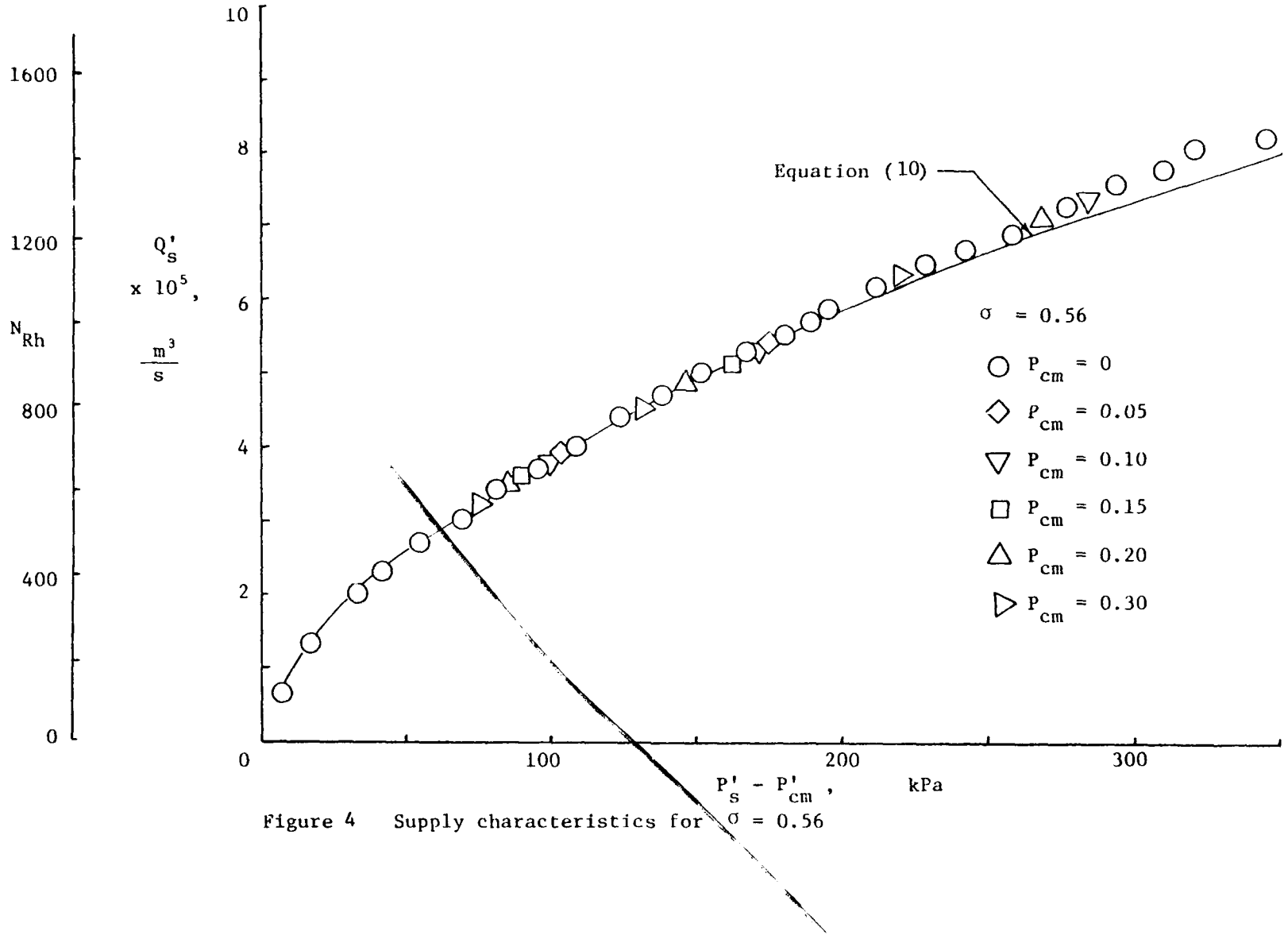

Figure 4 Supply characteristics for σ = 0.56

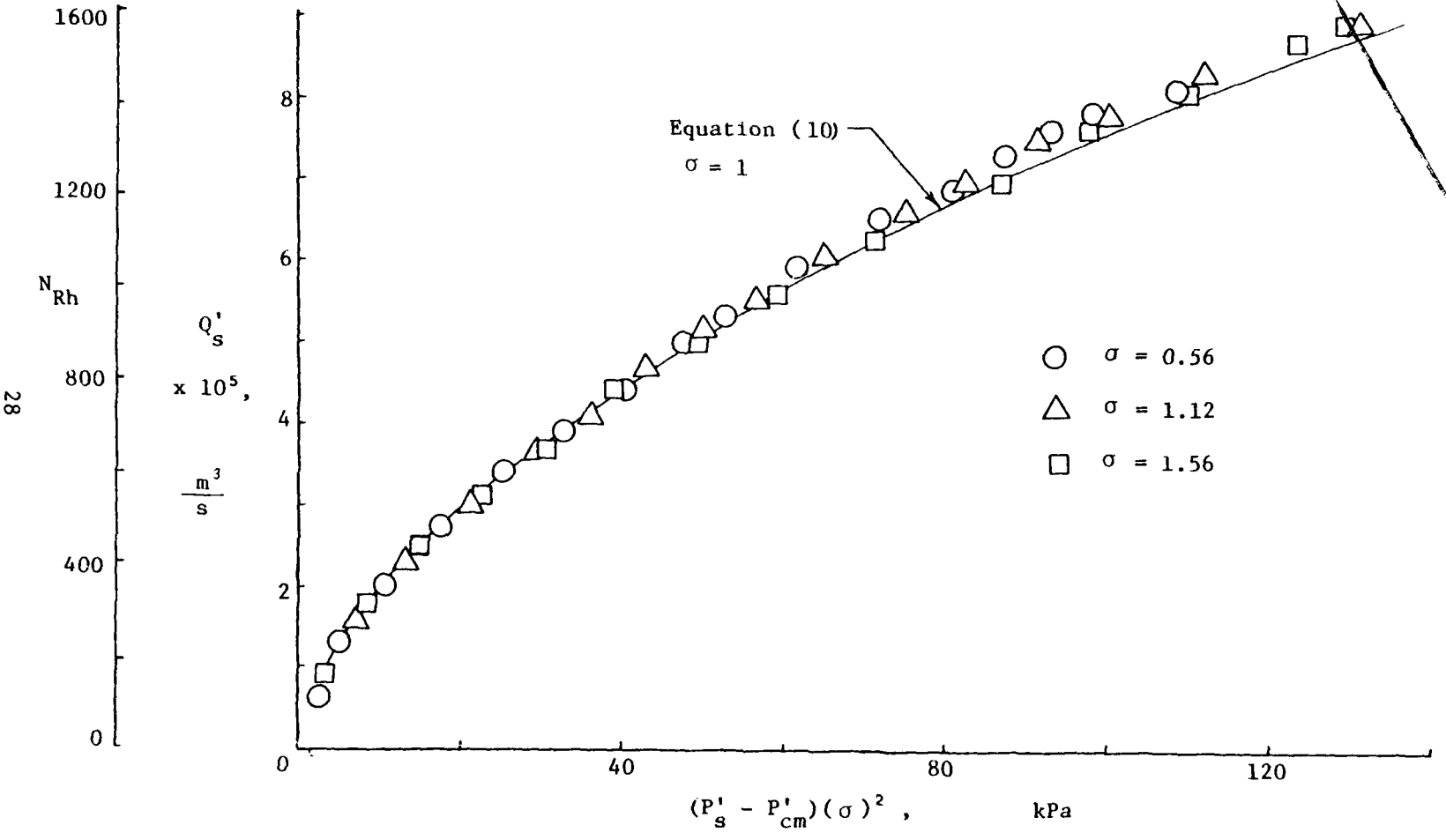

Figure 5 Supply characteristics for σ = 0.56; σ = 1.12; σ = 1.56

the aspect ratios are essentially the same as that shown. This figure is especially useful in the design of systems utilizing laminar amplifiers since a single curve is obtained for the relationship between the supply Reynolds number (or flow), supply pressure, and aspect ratio. Thus specification of two of these parameters easily yields the third parameter.

3.2 Input Characteristics

Figure 6 presents data on the input characteristics for both the null condition and the push-pull (i.e. $\delta P_{c2} = \delta P_{c1}$) deflected-jet condition for an aspect ratio of 1.12 and a Reynolds number of 1100. Data are presented for the deflected-jet pressure-flow characteristics for mean control pressures of 5, 10, 15, 20 and 30 per cent of the supply pressure. Also presented on this figure are the predicted pressure-flow characteristics for the null condition given by Eqn. (22) and for the push-pull condition given by Eqn. (30).

During this data acquisition and for all data to be presented, the supply pressure was held constant when investigating the effects of mean control pressure variation. Thus for a given supply pressure the supply flow rate and Reynolds number decreased as the mean control pressure was increased. The supply flow rate used in all flow rate normalization is that supply flow rate occurring for a zero mean control pressure. The Reynolds number appearing on all figures are the Reynolds numbers for zero mean control pressure.

The agreement between theory and data shown in Fig. 6 is noted to be quite satisfactory. As theory predicts the push-pull input resistance decreases with increasing mean control pressure. The push-pull data are observed to be essentially linear over the entire operating range. This observation indicates that the predicted push-pull characteristics, obtained from a linearized analysis, need not be restricted to the case of extremely small signal changes.

Data presented and discussed by Smith[4] on the input characteristics for aspect ratios of 0.56, 1.12 and 1.56 and for Reynolds numbers of 730 to 1400 indicate that the input characteristics do not demonstrate a strong dependendy on the aspect ratio or Reynolds number. The data for an aspect ratio of 0.56 indicated a lower deflected-jet input resistance than theory predicted.

Smith[4] also presents data on the deflected-jet input characteristics for low mean control pressures and for single-sided pressure (i.e. $\delta P_{c2}=0$) input signals as well as an analysis of the degree of cross-coupling exhibited by the LPA. He states that anomalies may occur in the deflected-jet input characteristics at low mean control pressures and that the supply jet may exhibit bistable characteristics at low mean control pressures where the null

---

[4]Smith, G. V., An Analysis of Laminar Proportional Amplifiers, Ph.D. Thesis, The Pennsylvania State University, University Park, PA., 1975.

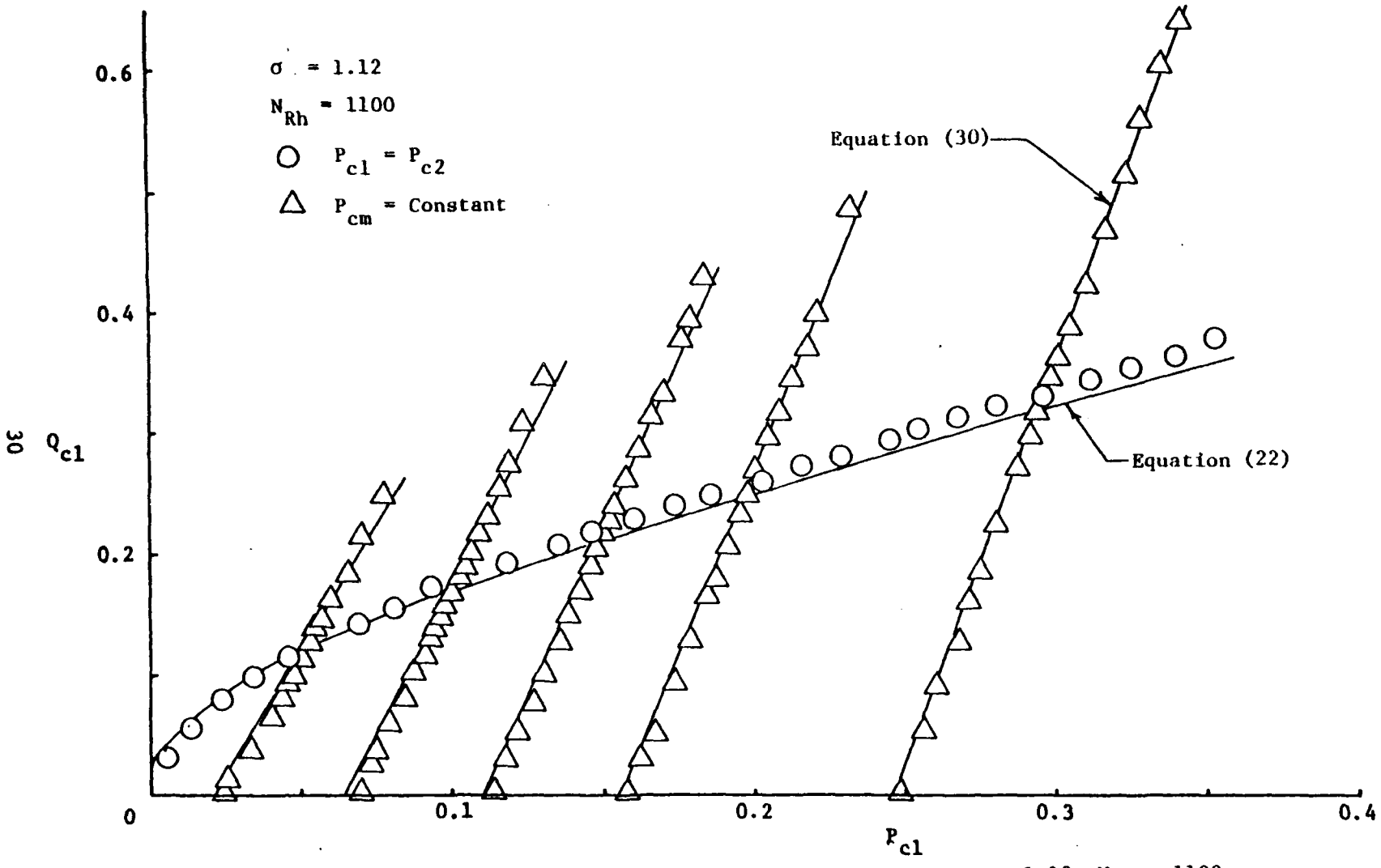

Figure 6. Null and push-pull input characteristis for σ = 1.12; N_{Rh} = 1100.

input resistance becomes very large. The LPA also indicated a high degree of cross-coupling existing between the control ports as the mean control pressure is increased above zero.

Since Smith and Shearer[2] discussed the possibility of satisfactory operation for setbacks less than one-half the supply nozzle width, data were taken on the input characteristics for a setback of one-fourth the supply nozzle width. These data are presented in Fig. 7 for an aspect ratio of 1.07 and a Reynolds number of 750. Data are also shown for a setback of one-half the supply nozzle width to facilitate interpretation of the effects of reduced setback. As is evident by this figure, the reduction in setback yields a greater null input resistance as theory predicts. However, both data and theory indicate that the push-pull input resistances are essentially the same for both values of setback at a given mean control pressure.

3.3 Transfer Characteristics

Figure 8 presents a typical set of transfer characteristics for an aspect ratio of 1.12, Reynolds number of 1100 and mean control pressure of 5, 10, 20 and 30 per cent of the supply pressure for a push-pull input signal under blocked-load conditions. From this figure and data for other aspect ratios and Reynolds numbers as presented by Smith[4] it is apparent that the pressure gain of the LPA decreases with increasing mean control pressure. For a given aspect ratio the decrease in pressure gain with increasing mean control pressure was found to be slightly more pronounced for the lower Reynolds numbers as theory predicts. The LPA is observed to exhibit relatively flat saturation characteristics. It was determined, however, that for each aspect ratio and Reynolds number a mean control pressure existed at which point the saturation characteristic would begin to droop. The linear range of operation was also found to increase slightly with increasing Reynolds number.

As might be expected the LPA model with a reduced setback exhibited a smaller operating range than the original model although the gain was essentially the same. It is important to note, however, that the range of operation of the reduced setback model included the original linear range of operation.

Figure 9 is a plot of the pressure gain versus the mean control pressure for aspect ratios of 0.56, 1.12 and 1.56. Also shown on this figure are the predicted gains for each aspect ratio. The data and theory indicate a decrease in the pressure gain as the mean control pressure is increased. At lower mean control pressures both data and theory predict a higher pressure

---

[2]Smith, G. V., and Shearer, J. L., Research Investigation on Laminar Proportional Amplifiers, Final Report Contract DAAG-39-72-C-0190, The Pennsylvania State University, University Park, PA., 1974.

[4]Smith, G. V., An Analysis of Laminar Proportional Amplifiers, Ph.D. Thesis, The Pennsylvania State University, University Park,PA., 1975.

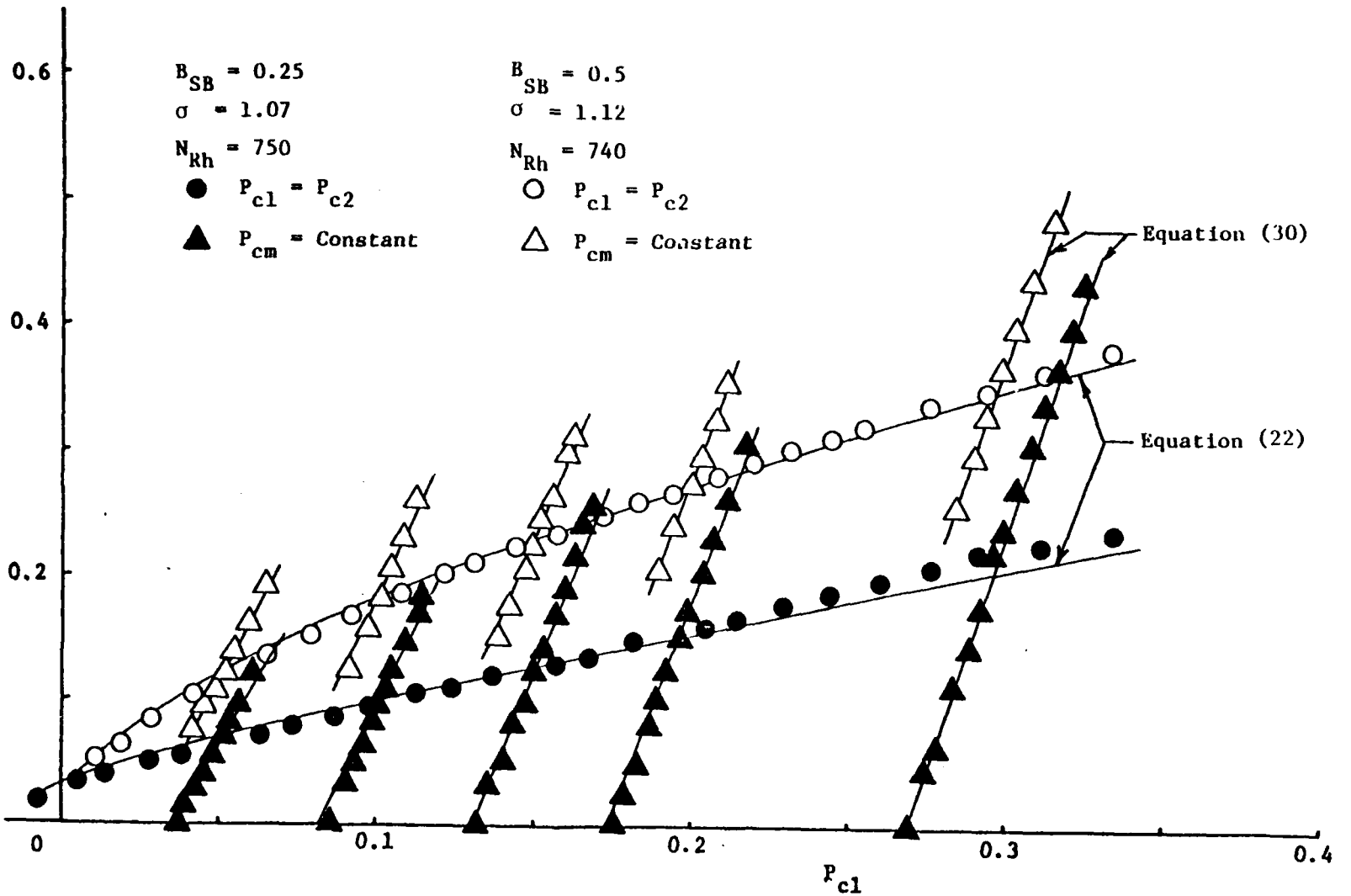

Figure 7. Null and push-pull input characteristics for B_{SB} = 0.25 and B_{SB} = 0.5.

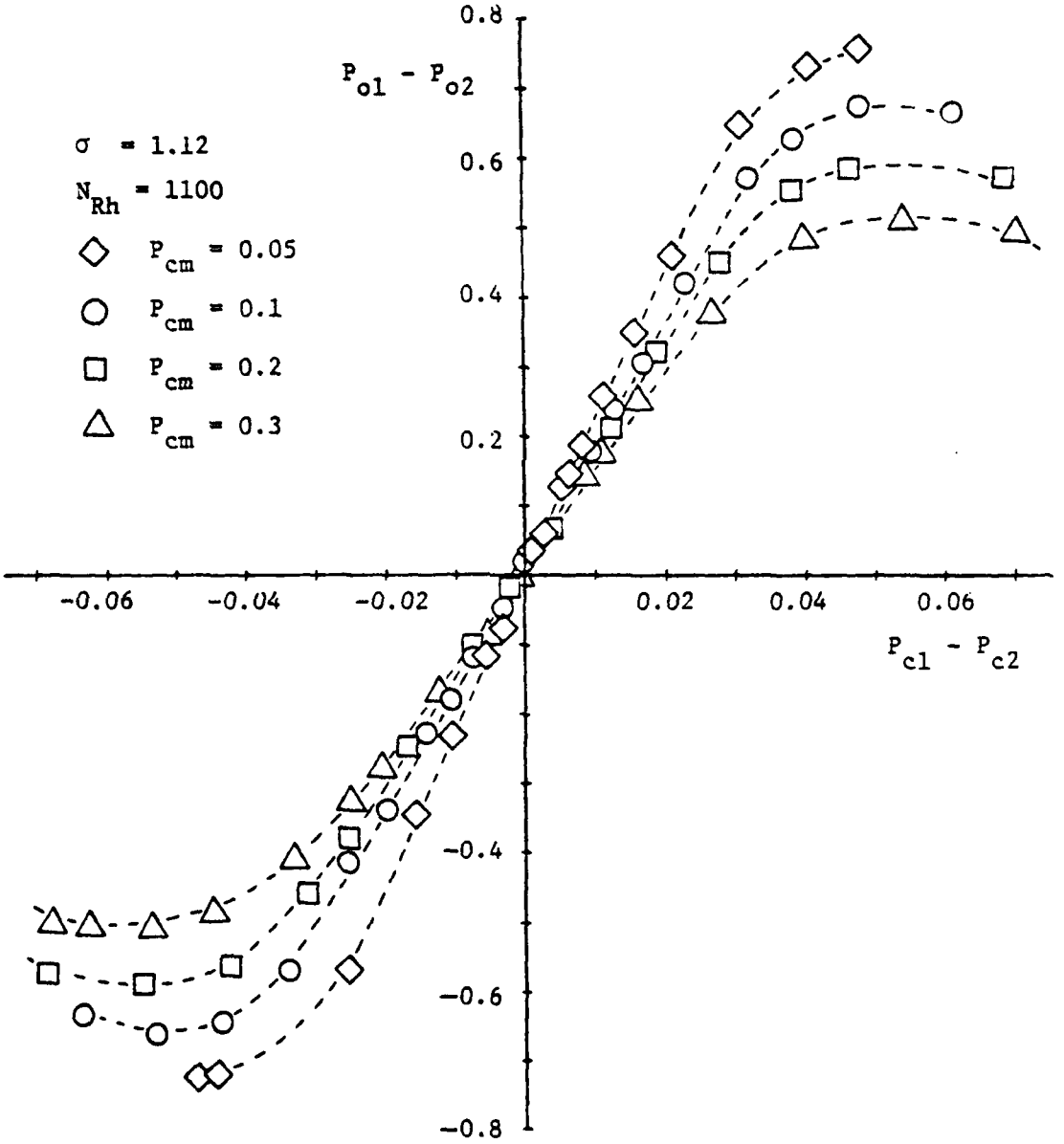

Figure 8. Push-pull transfer characteristics for σ = 1.12; N_{Rh} = 1100.

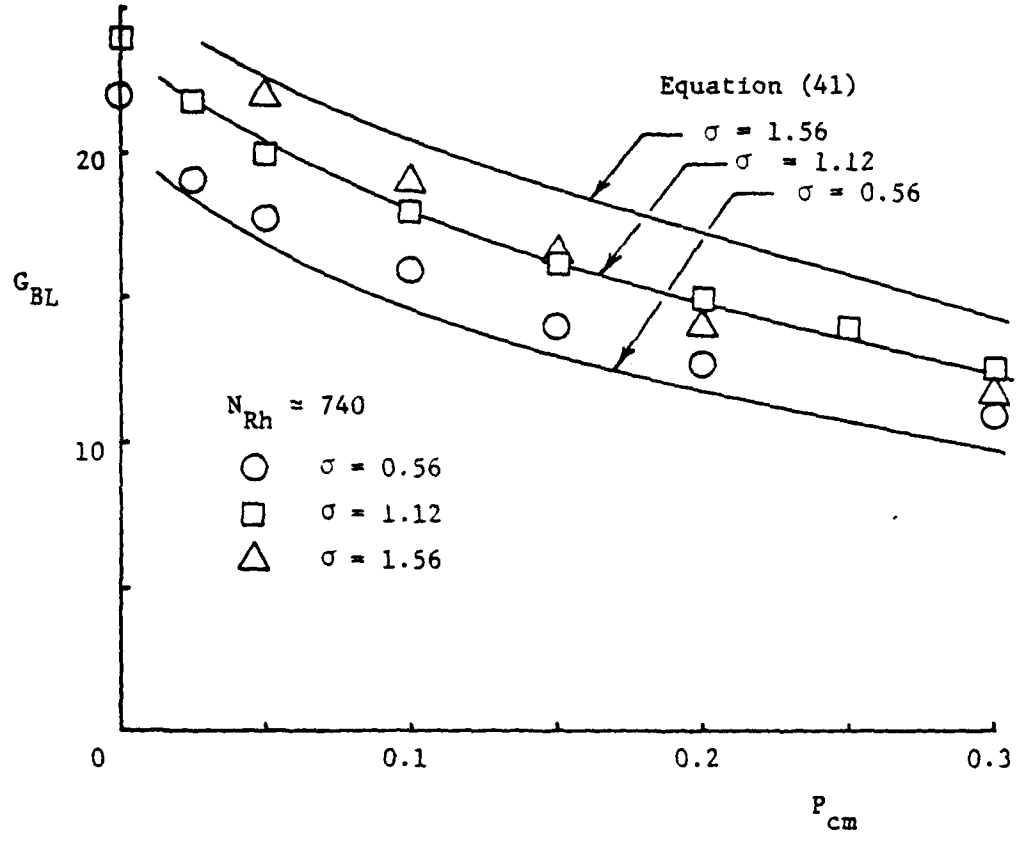

Figure 9. Blocked-load pressure gain variation with mean control pressure.

gain for the higher aspect ratios. It is noted, however, that the decrease in the pressure gain with increasing mean control pressure for an aspect ratio of 1.56 is greater than theory predicts. The theory is observed to predict a stronger aspect ratio dependency than the data indicates.

Figure 10 is a plot of the blocked-load pressure gain versus Reynolds number for a mean control pressure of 15 per cent of the supply pressure. Data for each of the aspect ratios are presented. The predicted pressure gain for an aspect ratio of unity is also presented in this figure. Theory predicts a pressure gain increase with increasing Reynolds number that is greater than the data indicate. It appears that the pressure gain begins to level off as the Reynolds number is increased. This, perhaps, is as would be expected since the pressure gain should reach a maximum at some value of Reynolds number and then decrease.

Although the transfer characteristics of proportional amplifiers are normally presented for blocked-load conditions, they are not, in general, operated under blocked-load conditions in actual applications. Thus data were taken on the pressure gain of the LPA for various equal resistive loads applied to the output ports.

The effect of applied output load resistance on the pressure gain of the LPA is more clearly understood if the pressure gain is normalized with respect to the blocked-load pressure gain and is plotted versus the incremental load resistance applied to the output ports for a particular aspect ratio and Reynolds number. Figure 11 presents this data for an aspect ratio of 1.12, Reynolds number of 1000 and for mean control pressures of 10, 15 and 20 per cent of the supply pressure. Although the blocked-load pressure gain has been shown to be a strong function of the mean control pressure, the effect of mean control pressure on the normalized gain is found to be small. The data presented in this figure indicate that for output resistive loads greater than approximately three times the supply resistance, the pressure gain of the LPA is essentially the same as for the blocked-load condition. Also presented on this figure is the predicted normalized gain calculated from Eqn. (47). Good agreement is noted to exist between the experimental data and the mathematical model predictions.

The information presented in Fig. 11 is especially useful in the design of systems utilizing laminar amplifiers since it may be possible to design the LPA so that the pressure gain is essentially independent of the output load. However, the fact is emphasized that both the incremental load resistance and apparent load resistance must be known before the pressure gain can be determined for given operating conditions. This is to say that the complete pressure-flow characteristics of the load to be driven by the LPA must be known. The data and theory presented in Fig. 11 are for a particular type of load (primarily of an orifice type) and care must be taken in applying the information presented in this figure to other types of applied loads.

3.4 Output Characteristics

A typical set of output characteristics are presented in Fig. 12 for equal resistive loads applied to the output ports and for various values of push-pull input signals. On this figure considerably more data are

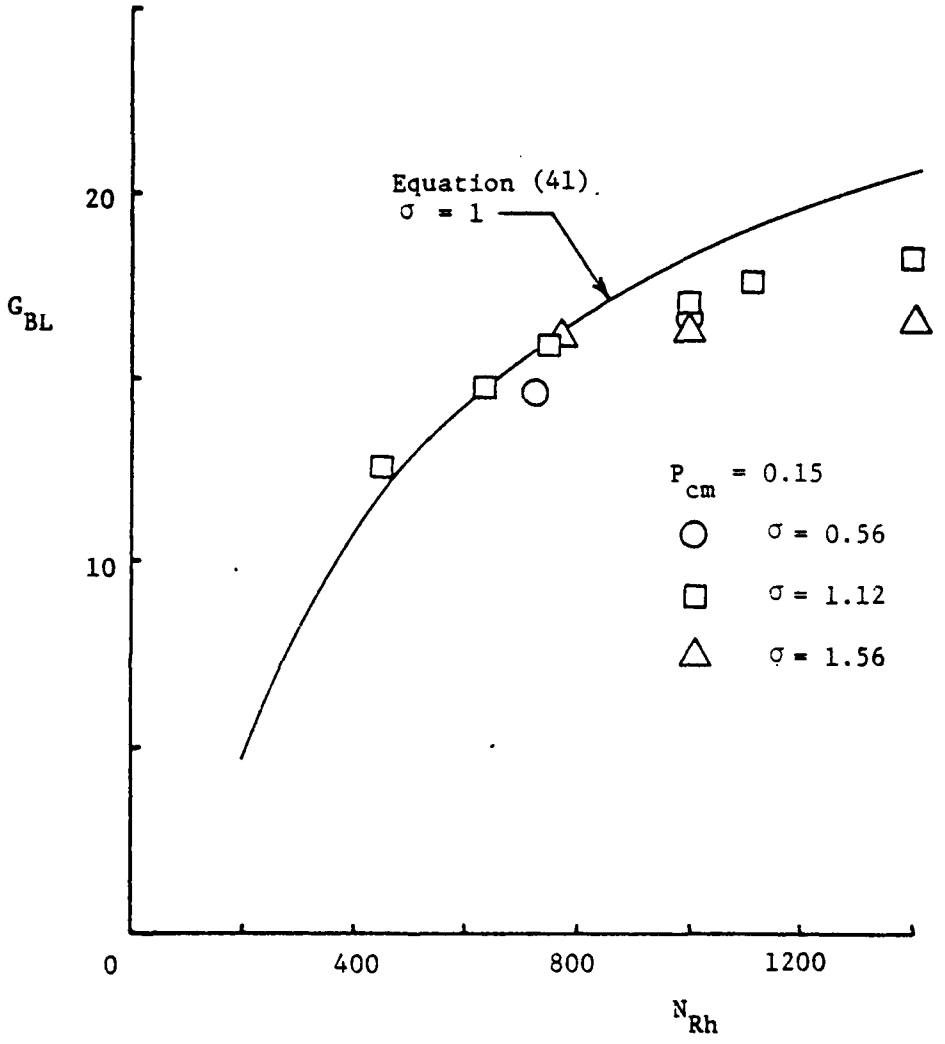

Figure 10. Variation of pressure gain under blocked-load conditions with Reynolds number.

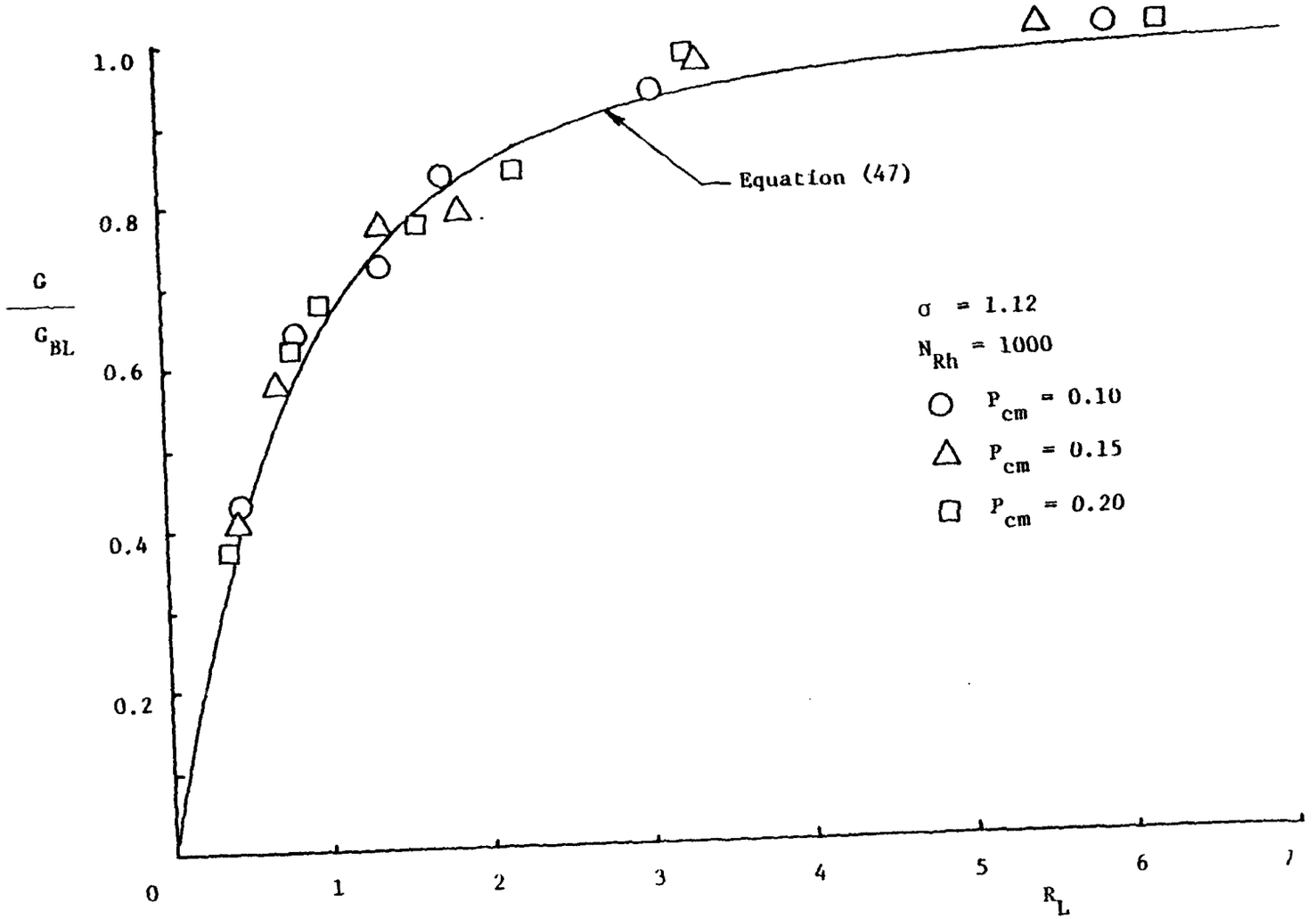

Figure 11. Normalized pressure gain versus output loading.

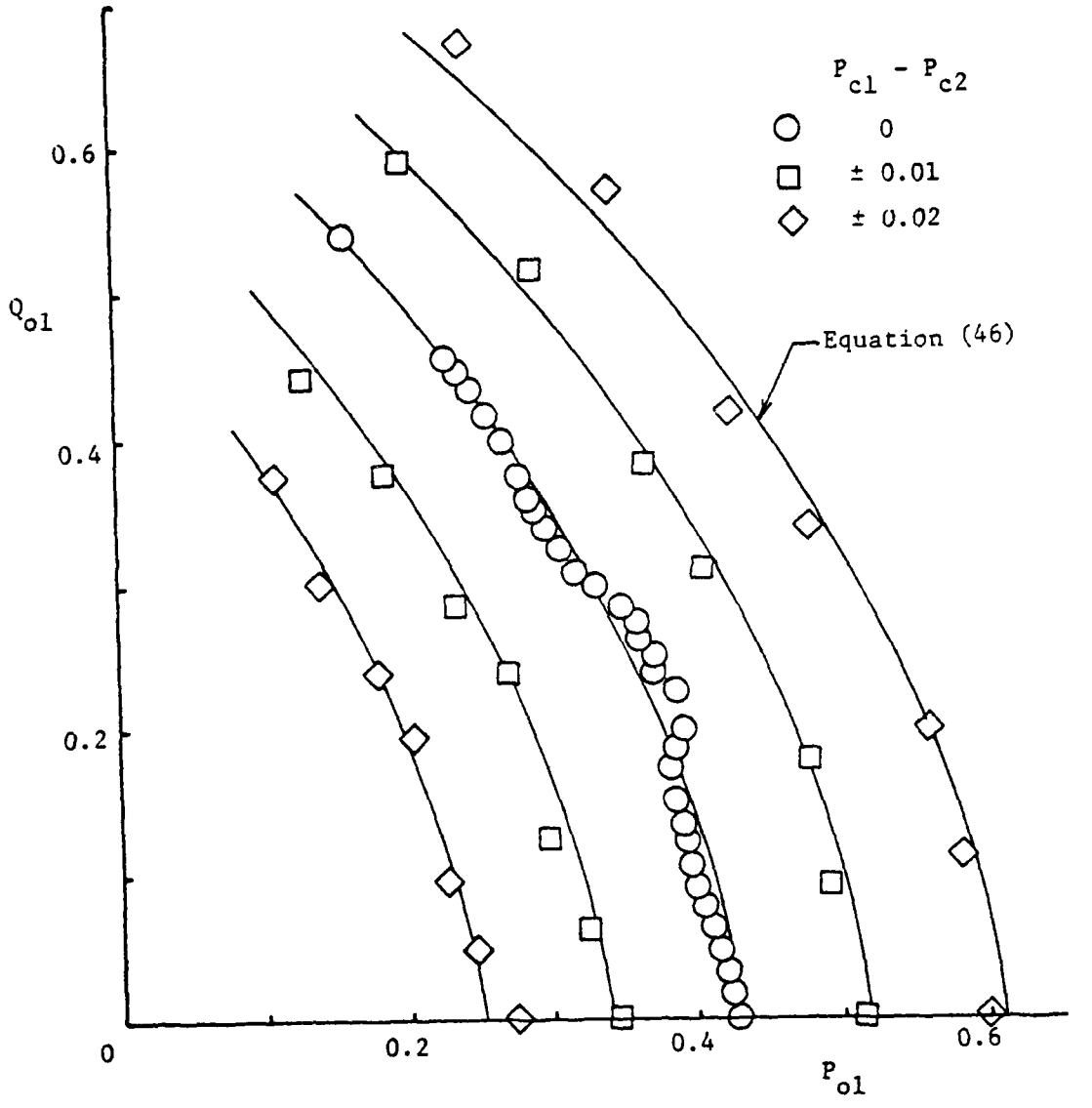

Figure 12. Output characteristics for σ = 1.12; N_{Rh} = 1000; P_{cm} = 0.15.

presented for the null condition since during repeatability tests it was observed that the output characteristic data points did not fall along as smooth a curve as was originally thought. Thus, the data were repeated with considerably closer spacing of data points for the null condition. Also shown on this figure are the predicted output characteristics calculated from Eqn. (46). Reasonable agreement is noted to exist between theory and data although the data do not fall along as smooth a curve as theory predicts. The deflected-jet data follow the same trend as the null condition data. This anomaly in the output characteristics was also found to exist for other values of mean control pressure as discussed by Smith.[4] Smith[4] also presents data for other aspect ratios, Reynolds numbers, mean control pressures and output loading conditions. He reports that a considerable amount of cross-coupling exists between the output ports and that anomalies can occur in the output characteristics.

3.5 Differential Output Noise

The true RMS value of the fluctuating component of the differential output pressure was measured for a bandwidth of 0 to 200 Hz. A portion of this data for a mean control pressure of 15 per cent of the supply pressure is presented in Fig. 13 which indicates that the differential output pressure noise increases proportionally with aspect ratio and exponentially with Reynolds number. Smith[4] also presents data on both the true RMS value and the power spectral density of the fluctuating component of the differential output pressure for various aspect ratios, Reynolds number and mean control pressures. Generally it was observed that the differential output pressure noise was a minimum for mean control pressures around 15 per cent of the supply pressure and that the major components of the pressure noise were concentrated in the low frequency spectrum.

4. CONCLUSIONS

Based on the results of this study it is concluded that the use of pressure-controlled amplifiers operating with laminar supply jets can offer certain advantages over amplifiers operating in the turbulent supply jet regime. Some of these advantages include: 1) significant increase in pressure gain; 2) significant increase in signal-to-noise ratios; 3) reduced power consumption; 4) stable operation under blocked-load conditions; 5) decreased output resistance.

Some of the disadvantages of the LPA as compared to typical amplifiers operating with turbulent supply jets include: 1) significant decrease in both the null input resistance and deflected-jet input resistance; 2) strong dependency of the amplifiers performance on the mean control pressure; and 3) high degree of cross-coupling between control ports.

---

[4]Smith, G. V., An Analysis of Laminar Proportional Amplifiers, Ph.D. Thesis, The Pennsylvania State University, University Park, PA., 1975.

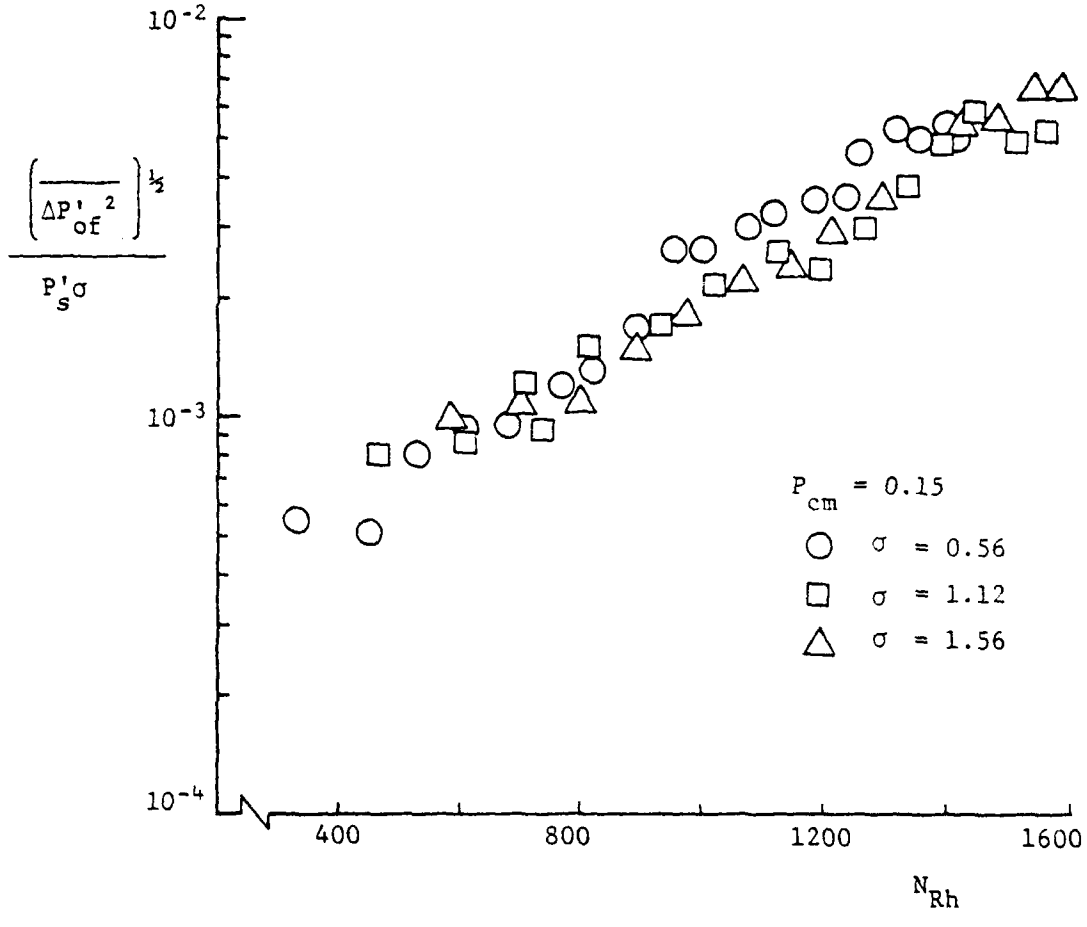

Figure 13. Differential output noise as a function of Reynolds number.

It was shown, however, that the null input resistance could be significantly increased by a reduction in the setback of the control knife-edges from 0.5 B'_s to 0.25 B'_s . It was determined that the reduction in operating range resulting from this reduced setback did not affect appreciably the linear range of operation.

In general, acceptable agreement between the experimental data and the predicted characteristics was observed--verifying, to a certain degree, the range over which the model is reasonably valid. However, the mathematical model was found to predict a stronger dependency on the aspect ratio than was observed experimentally.

An analysis of the differential output noise indicated an exponential growth of the noise with increasing Reynolds number. Thus, low Reynolds number operation may be desirable for applications where low output noise is important.

REFERENCES

1. Manion, F. M., and Mon, G., Fluerics: 33. Design and Staging of Laminar Proportional Amplifiers, Harry Diamond Laboratories-TR-1608, Adelphi, MD, 1972.

2. Smith, G. V., and Shearer, J. L., Research Investigation on Laminar Proportional Amplifiers, Final Report Contract DAAG-39-72-C-0190, The Pennsylvania State University, University Park, PA., 1974.

3. Manion, F. M., and Drzewiecki, T. M., Analytic Design of Laminar Proportional Amplifiers, Proceedings HDL Fluidics State-of-the Art Symposium, Adelphi, MD, 1974.

4. Smith, G. V., An Analysis of Laminar Proportional Amplifiers, Ph.D. Thesis, The Pennsylvania State University, University Park, PA., 1975.

5. Schlicting, H. Boundary Layer Theory, McGraw-Hill Book Co., Inc., N. Y. 1968.

6. Sparrow, E. M., Hixon, C. W., and Shavit, G., Experiments on Laminar Flow Development in Rectangular Ducts, Trans. ASME, Journal of Basic Engineering, Vol. 89, 1967.

7. Shapiro, A. H., Siegel, R., and Kline, S. J., Friction Factors in the Laminar Entry Region of a Smooth Tube, Proc. U. S. Nat. Congr. Appl. Mech., 1954.

8. Han, L. S., Hydrodynamic Entrance Lengths for Incompressible Laminar Flow in Rectangular Ducts, Trans. ASME, Journal of Applied Mechanics, Vol. 82, 1960.

9. Ehrich, F. F., Some Hydrodynamic Aspects of Valves, ASME Paper No. 55-A-114, 1955.

Fluidics Distribution List

Commander IDDR & E
Pentagon, Room 3D 1089
Washington, DC 20310
ATTN: Dr. David A. Charvonia
ATTN: Dr. Leonard Weisberg

Defense Documentation Center
Cameron Station, Building 5
Alexandria, VA 22314
ATTN: DDC-TO 12 copies

Office of the Deputy Chief of Staff for
Research, Development & Acquisition
Department of the Army
Washington, DC 20310
ATTN: DAMA-ARP-P, Dr. V. Garber
ATTN: Major P. Tate, Rm 3D424

US Army R&D Group (Europe)
Box 15
FPO New York 09510
ATTN: Chief, Aeronautics Branch
ATTN: Chief, Engineering Sciences

US Army Research Office
P. O. Box 12211
Research Triangle Park, NC 27709
ATTN: James J. Murray, Eng Sci Div
ATTN: Dr. Robert Singleton

Commander
HQ, US Army Materiel Command
5001 Eisenhower Avenue
Alexandria, VA 22333
ATTN: AMCRD-TP, William Ralph
ATTN: AMCRD-TP, J. Corrigan

Commander
USA Foreign Science & Technology Center
Federal Office Building
220 7th Street N.E.
Charlottesville, VA 22901
ATTN: AMXST-IS3, C. R. Moore

Director
Eustis Directorate
USA Air Mobility Rsch & Dev Lab
Fort Eustis, VA 23604
ATTN: George W. Fosdick, SAVDL-EU-SYA

Commander
USA Missile Command
Redstone Arsenal, AL 35809
ATTN: Redstone Scientific Information Center, AMSMI-RBD
ATTN: AMSMI-RGC, William Griffith
ATTN: AMSMI-RGC, James G. Williams
ATTN: AMSMI-RGC, J. C. Dunaway
ATTN: AMCPM-TOW, (Fred J. Cheplen)

Commander
USA Mobility Equipment R&D Center
Fort Belvoir, VA 22060
ATTN: Technical Library (Vault)
ATTN: SMEFB-O, R. N. Ware

Commander
Edgewood Arsenal
Aberdeen Proving Ground, MD 21010
ATTN: SAREA-MT-T (Mr. D. Patton)

Commander
Picatinny Arsenal
Dover, NJ 07801
ATTN: SARPA-ND-C-C (D. Sampar)
ATTN: SARPA-TS-S-#59
ATTN: SARPA-ND-C-C (A. E. Schmidlin)

Commander
Watervliet Arsenal
Watervliet Arsenal, NY 12189
ATTN: Gary W. Woods
ATTN: SARWV-RDT-L
ATTN: John Barrett

Commander
USA Tank Automotive Command
Armor & Comp Div, AMSTA-RKT
Bldg. 215
Warren, MI 48090
ATTN: T. Kozowyk
ATTN: M. Steele

Commander
White Sands Missile Range, NM 88002
ATTN: STEWS-AD-L, Technical Library

Commander
US Army Armament Command
Rock Island, IL
ATTN: AMSAR-RDG-T (Mr. R. Spencer)
ATTN: AMSAR-ASF

Commander
Rodman Laboratories
Rock Island Arsenal
Rock Island, IL 61201
ATTN: SARRI-LA

Office of Naval Research
Department of the Navy
Arlington, VA 22217
ATTN: Stanley W. Doroff, Code 438
ATTN: D. S. Siegel, Code 211

Commander
Naval Air Development Center
Warminster, PA 18974
ATTN: Horace B. Welk, Jr. (30424)
ATTN: Code 8134, Lois Guise

Commanding Officer
Naval Air Engineering Center
Lakehurst, NY 08733
ATTN: ESSD, Code 9314, Harold Ott

Naval Air Systems Command
Code: Air-52022A (J. Burns)
Dept. of the Navy
Washington, DC 20360

Commander
Pacific Missile Range
Naval Missile Center
Point Mugu, CA 93042
ATTN: Abe J. Garrett, Code 4121.2
ATTN: Code 4121, Charles Busenkell

Commander
Naval Ship Engineering Center
Philadelphia Division
Philadelphia, PA 19112
ATTN: Code 6772, D. Keyser

Commander
Naval Surface Weapons Center
White Oak, Md 20910
ATTN: Clayton McKindra, Code 413
ATTN: Div. 412, C. J. Sewell

Naval Postgraduate School
Mechanical Engineering
Monterey, CA 93940
ATTN: Prof. T. Sarpkaya

Naval Ship Res & Dev Center
Code 5641
Bethesda, Md 20084

Naval Sea Systems Command
SEA0331H
Washington, DC 20362
ATTN: A. Chaikin

Commander
Naval Weapons Center
China Lake,CA 93555
ATTN: Code 533, Library Division

Commander
AF Aero Propulsion Laboratory, AFSC
Wright-Patterson AFB, OH 45433
ATTN: Lester Small lTBC

Commander
Air Force Avionics Lab
Wright-Patterson AFB, OH 45433
ATTN: RWN-2 (Richard Jacobs)

Director
AF Office of Scientific Research
1400 Wilson Blvd
Arlington, VA 22209
ATTN: NE (Mr. George Knausenberger)

Commander
Air Force Flight Dynamics Laboratory
ATTN: FDCL (H. Snowball)
Wright-Patterson AFB, OH 45433

Commander
AF Weapons Laboratory, AFSC
Kirtland AFB, NM 87117
ATTN: SUL, Technical Library

Commander
Armament Development and Test Center
Eglin Air Force Base, FL 32542
ATTN: ADTC (DLOSL), Tech Library

Air Force Flight Test Center
6510 ABG/SSD
Edwards AFB, CA 93523
ATTN: Technical Library

4950th Test Wing (TZHM)
Wright-Patterson Air Force Base
Dayton, OH 45424
ATTN: Mr. Michael Collins

AF Institute of Technology, AU
Wright-Patterson AFB, OH 45433
ATTN: Library AFIT(LD), Bldg. 640, Area B
ATTN: AFIT(ENM), Milton E. Franke (3 copies)

USAF School of Aerospace Medicine
ATTN: USAFSAM/VNT, Capt. Paul Zalesky
Brooks AFB, TX 78235

US Atomic Energy Commission
Washington, DC 20545
ATTN: RDT, F. C. Legler

Oak Ridge National Laboratory
Central Res Library, Bldg 4500N, Rm. 175
P.O. Box X
Oak Ridge, TN 37830
ATTN: E. Howard

Department of Commerce
Bureau of East-West Trade
Office of Export Administration
Washington, DC 20230
ATTN: Walter J. Rusnack

Scientific Library
US Patent Office
Washington, DC 20231
ATTN: Mrs. Cureton

Department of Commerce
National Bureau of Standards
Washington, DC 20234
ATTN: Gustave Shapiro, 425.00

NASA Ames Research Center
Moffett Field,CA 94035
ATTN: MS 244-13, Dean Chisel

NASA Langley Research Center
Hampton, VA 23665
ATTN: H. D. Garner, MS 494
ATTN: R. R. Hellbaum, MS 494
ATTN: MS 185, Technical Library

NASA Lewis Research Center
21000 Brookpark Road
Cleveland, OH 44135
ATTN: Vernon D. Gebben

NASA Scientific & Tech Info Facility
P. O. Box 8657
Baltimore/Washington International Airport, MD 21240
ATTN: Acquisitions Branch

University of Alamba
Civil & Mineral Engineering Dept.
P. O. Box 1468
University, AL 35486
ATTN: Dr. Harold R. Henry

Arizona State University
Engineering Center
Tempe, AZ 85281
Laboratory for Measurement Systems Engineering
ATTN: Peter K. Stein

University of Arkansas
Technology Campus
P. O. Box 3017
Little Rock, AR 72203
ATTN: Paul C. McLeod

University of Arkansas
Mechanical Engineering
Fayetteville, AR 72701
ATTN: Jack H. Cole, Assoc Prof

Carnegie-Mellon University
Schenley Park
Pittsburgh,PA 15213
ATTN: Prof W. T. Rouleau, Mech. Engr Dept

Case Western Reserve University
University Circle
Cleveland, OH 44106
ATTN: Prof P. A. Orner

The City College of the City Univ. of NY
Dept of Mech Engr
139th St. at Convent Ave
New York, NY 10031
ATTN: Prof. L. JiJi
ATTN: Prof. G. Lowen

Duke University
College of Engineering
Durham, NC 27006
ATTN: C. M. Harman

Engineering Societies Library
345 East 47th Street
New York, NY 10017
ATTN: Howard Gordon

Franklin Institute of the State of Pennsylvania
20th Street & Parkway
Philadelphia, PA 19103
ATTN: Ka-Cheung Tsui, Elec Engr Div
ATTN: C. A. Belsterling

IIT Research Institute
10 West 35th Street
Chicago, IL 60616
ATTN: Dr. K. E. McKee

Lehigh University
Department of Mechanical Engineering
Bethlehem, PA 18015
ATTN: Prof Forbes T. Brown

Linda Hall Library
5109 Cherry Street
Kansas City, MO 64110
ATTN: Documents Division

Massachusetts Institute of Technology
77 Massachusetts Avenue
Cambridge, MA 02139
ATTN: Engineering Technical Reports, RM 10-408
ATTN: David Wormley, Mech Engr Dept.
Room 3-146

Michigan Technological University
Library, Documents Department
Houghton, MI 49931
ATTN: J. Hawthorne

Milwaukee School of Engineering
Fluid Power Institute
1025 N. Milwaukee St
Milwaukee, WI 53201
ATTN: K. Johnson

University of Mississippi
201 Carrier Hall, Dept of Mech Engr
University, MS 38677
ATTN: Dr. John A. Fox

Mississippi State University
Drawer ME
State College, MS 39672
ATTN: Dr. C. J. Bell, Mech Eng Dept

University of Nebraska Libraries
Acquisitions Dept. Serials Section
Lincoln, Nebraska 68508
ATTN: Alan Gould

University of New Hampshire
Mech. Engr Dept. Kingsbury Hall
Durham, NH 03824
ATTN: Prof Charles Taft 3 copies

Ohio State University Libraries
Serial Division, Main Library
1858 Neil Avenue
Columbus, OH 43210

Oklahoma State University
School of Mech & Aerospace Engineering
Stillwater, OK 74074
ATTN: Prof Karl N. Reid

Pennsylvania State University
Dr. J. L. Shearer
215 Mechanical Engineering Building
University Park, PA 16802

Pennsylvania State University
Engineering Library
201 Hammond Bldg.
University Park,PA 16802
ATTN: M. Bennett, Engineering Librarian

Purdue University
School of Mechanical Engineering
Lafayette, IN 47907
ATTN: Prof. Victor W. Goldschmidt
ATTN: Prof. Alan T. McDonald

Rock Valley College
3301 North Mulford Road
Rockford, IL 61101
ATTN: Ken Barton

Rutgers University
Library of Science & Medicine
New Brunsic, NJ 08903
Government Documents Dept
ATTN: Ms. Sandra R. Livingston

Syracuse University
Dept of Mech & Aerospace Engineering
139 E. A. Link Hall
Syracuse, NY 13210
ATTN: Professor D. S. Dosanjh

University of Texas at Austin
Dept of Mechanical Engineering
Austin,TX 78712
ATTN: Dr. A. J. Healey

Tulane University
Dept. of Mechanical Engineering
New Orleans, LA 70118
ATTN: H. F. Hrubecky

Union College
Mechanical Engineering
Schenectady, NY 12308
ATTN: Assoc Prof W. C. Aubrey
Mech Engr Dept, Steinmetz Hall

Washington University
School of Engineering
P.O. Box 1185
St. Louis, MO 63130
ATTN: W. M. Swanson

West Virginia University
Mechanical Engineering Department
Morgantown, WV 26505
ATTN: Dr. Richard A. Bajura

Wichita State University
Wichita, KS 67208
ATTN: Dept Aero Engr, E. J. Rodgers

University of Wisconsin
Mechanical Engineering Department
1513 University Avenue
Madison, WI 53706
ATTN: Federal Reports Center
ATTN: Norman H. Beachley, Dir,
Design Engineering Laboratories

Worcester Polytechnic Institute
Worcester, MA 01609
ATTN: George C. Gordon Library (TR)
ATTN: Technical Reports

AiResearch
P. O. Box 5217
402 South 36th Street
Phoenix, AZ 85034
ATTN: David Schaffer

Avco Systems Division
201 Lowell Street
Wilmington, MA 01887
ATTN: W. K. Clark 2 copies

Bell Helicopter Company
P. O. Box 482
Forthworth, TX 76101
ATTN: Jerry C. Bryant

Bendix Corporation
Research Laboratories Div.
Bendix Center
Southfield, MI 48075
ATTN: Andrew Seleno
ATTN: C. J. Ahern

Boeing Company, The
P.O. Box 3707
Seattle, WA 98124
ATTN: Henrik Straub

Bowles Fluidics Corporation
9347 Fraser Avenue
Silver Spring, MD 20910
ATTN: P. Bauer, Vice President/Engineering

Continental Can Co.
Tech Center
1350 W. 76th Street
Chicago, IL 60620
ATTN: P. A. Bauer

Cardis Corporation
P.O. Box 428
Miami, FL 33137
ATTN: Stephen F. Vadas, K-2

Corning Glass Works
Fluidic Products, Houghton Park, B-2
Corning, NY 14830
ATTN: W. T. Greenfield

EMX Engineering, Inc.
354 Newark-Pompton Turnpike
Wayne, NJ 07470
ATTN: Anthony P. Corrado, President

Fluidics Quarterly
P.O. Box 2989
Stanford, CA 94305
ATTN: D. H. Tarumoto

General Electric Company
Space/RESD Divisions
P.O. Box 8555
Philadelphia, PA. 19101
ATTN: Mgr Libraries, Larry Chasen

General Electric Company
Specialty Fluidics Operation
Bldg 37, Room 523
Schenectady, NY 12345
ATTN: F. S. Ralbovsky, Fluidic Control
Products Engr.

General Electric Company
Specialty Fluidics Operation
Building 37, Room 523
Schenectady, NY 12345
ATTN: R. C. Kumpitsch, Manager Fluidic
Controls

General Motors Corporation
Delco Electronics Div
Manfred G. Wright
New Commercial Products
P.O. Box 1104
Kokomo, IN 46901
ATTN: R. E. Sparks

Grumman Aerospace Corporation
Technical Information Center
South Oyster Bay Road
Bethpage, L.I., NY 11714
ATTN: C. W. Turner, Documents Librarian

Honeywell, Inc.
1625 Zarthan Ave
Minneapolis, MI 55413
ATTN: Dick Evans, M.S. S2658

Johnson Controls, Inc.
507 E. Michigan
Milwaukee, WI 53201
ATTN: Warren A. Lederman

Martin Marietta Corporation
Aerospace Division
P.O. Box 5837
Orlando, FL 32805
ATTN: R. K. Broderson, MP 326
ATTN: Vito O. Bravo, MP 326

National Fluid Power Association
3333 North Mayfair Road
Milwaukee, WI 53222
ATTN: John R. Lueke
Dir of Tech Services

Richard White & Associates
Electro/Mechanical Engineers
77 Pelham Isle Road
Sudsbury, MA 01776
ATTN: Richard P. White

Rockwell International Corporation
Columbus Aircraft Division, P.O. Box 1259
4300 E 5th Avenue
Columbus, OH 43216
ATTN: Mr. Marvin Schweiger

Sandia Corporation
Kirtland AFB, East
Albuquerque, NM 87115
ATTN: William R. Leuenberger, Div 2323

United Technologies Research Center
400 Main Street
E. Hartford, CT 06108
ATTN: R. E. Olson, Mgr Fluid Dynamics
Laboratory

Harry Diamond Laboratories
ATTN: Einsel, David W., Col., Commanding
Officer/Carter, W. W./Sommer, H.
Marcus, S. M., Technical Director
ATTN: Kimmel, S., PIO
ATTN: Chief, 0021
ATTN: Chief, 0022
ATTN: Chief, Lab 100
ATTN: Chief, Lab 200
ATTN: Chief, Lab 300

ATTN: Chief, Lab 400
ATTN: Chief, Lab 500
ATTN: Chief, Lab 600
ATTN: Chief, Lab 700
ATTN: Chief, Lab 800
ATTN: Chief, Lab 900
ATTN: Chief, Lab 1000
ATTN: Chief, 041
ATTN: HDL Library 3 copies
ATTN: Chiarman, Editorial Committee 4 copies
ATTN: Chief, 047
ATTN: Tech Reports, 013
ATTN: Patent Law Branch, 071
ATTN: Chief, 340 25 copies
ATTN: Unit, 320